

Diastereoselective Coordination of P-Stereogenic Secondary Phosphines in Copper(I) Chiral Bis(phosphine) Complexes: Structure, Dynamics, and Generation of Phosphido Complexes

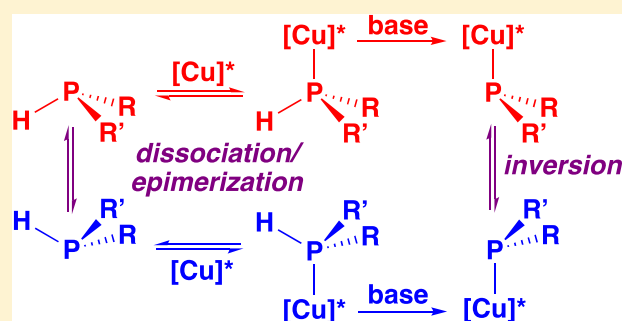
Sarah K. Gibbons,[†] Christopher R. D. Valleau,[†] Jesse L. Peltier,[†] Matthew F. Cain,[†] Russell P. Hughes,[†] David S. Glueck,^{*,†} James A. Golen,[‡] and Arnold L. Rheingold[‡]

[†]6128 Burke Laboratory, Department of Chemistry, Dartmouth College, Hanover, New Hampshire 03755, United States

[‡]Department of Chemistry, University of California, San Diego, 9500 Gilman Drive, La Jolla, California 92093, United States

Supporting Information

ABSTRACT: Diastereoselective coordination of racemic secondary phosphines (PHRR') to Cu(I) precursors containing chiral bis(phosphines) (diphos*) was explored as a potential route to P-stereogenic phosphido complexes. Reaction of [Cu(NCMe)₄][PF₆] with chiral bis(phospholanes) gave [Cu(diphos*)₂][PF₆] (diphos* = (R,R)-Me-DuPhos (1), (R,R)-Et-DuPhos (2), or (R,R)-Me-FerroLANE (3)) or the mono(chelates) [Cu(diphos*)(NCMe)_n][PF₆] (diphos* = (R,R)-i-Pr-DuPhos, n = 2 (4); diphos* = (R,R)-Me-FerroLANE, n = 1 (5)). Treatment of [Cu(NCMe)₄][PF₆] with diphos* and PHMe(Is) (Is = 2,4,6-(i-Pr)₃C₆H₂) gave mixtures of diastereomers of [Cu((R,R)-i-Pr-DuPhos)(PHMe(Is))(NCMe)][PF₆] (6) and [Cu((R,R)-Me-FerroLANE)(PHMe(Is))][PF₆] (7); two of the three expected isomers of the bis(secondary phosphine) complexes [Cu((R,R)-i-Pr-DuPhos)(PhHP(CH₂)_nPhPh)][PF₆] (n = 2 (8); n = 3 (9)) were formed preferentially in related reactions. Reaction of the halide-bridged dimers [Cu((R,R)-i-Pr-DuPhos)(X)₂] or [Cu((R,R)-Me-FerroLANE)(I)₂] with PHMe(Is) gave the labile adducts Cu((R,R)-i-Pr-DuPhos)(PHMe(Is))(X) (X = Cl (10), Br (11), I (12)) and Cu((R,R)-Me-FerroLANE)(PHMe(Is))(I) (13). Complexes 1, 6, and 8–11 were structurally characterized by X-ray crystallography. Variable temperature NMR studies of 6 and 8 showed that the secondary phosphine ligands underwent reversible dissociation. Deprotonation of 6 or 7 generated the P-stereogenic phosphido complexes Cu(diphos*)(PMeIs) (diphos* = (R,R)-i-Pr-DuPhos (14) or (R,R)-Me-FerroLANE (17)), observed by ³¹P NMR spectroscopy, but decomposition also occurred. Density functional theory calculations were used to characterize the diastereomers of thermally unstable 17 and the inversion barrier in a model copper-phosphido complex. These observations provided structure–property relationships which may be useful in developing catalytic asymmetric reactions involving secondary phosphines and P-stereogenic copper phosphido intermediates.



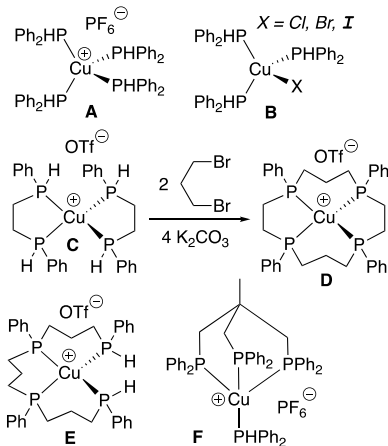
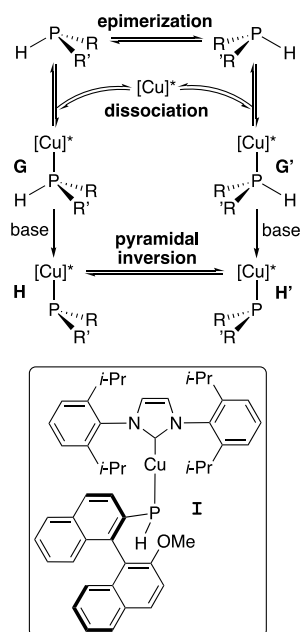
INTRODUCTION

The enhanced reactivity of the P–H bond in metal complexes of secondary phosphines has been exploited in both stoichiometric and catalytic P-alkylation.¹ Coordination of secondary phosphines to labile Cu(I),² as in cation **A** and neutral halide complexes **B** (Scheme 1),³ is potentially useful because rapid ligand substitution increases catalytic turnover frequency, limits product inhibition, and enables dechelation of macrocycles formed via P-alkylation.¹ For example, deprotonation/alkylation of **C** yielded macrocycle **D**, which was removed from copper as the phosphine oxide using H₂S in air.⁴ Similar base-mediated macrocyclization in **E** yielded tetradentate ligands, which were demetalated with KCN.⁵ Cation **F** is a rare example of a copper secondary phosphine complex involved in a catalytic cycle, alkylation of diphenylphosphine with benzyl halides or CH₂Cl₂; its deprotonation gave the unstable Cu-phosphido intermediate Cu(triphos)(PPh₂).⁶

Related *asymmetric* alkylation of secondary phosphines catalyzed by chiral precious metal complexes has been used to prepare enantiomerically enriched P-stereogenic phosphines, privileged ligands in homogeneous catalysis.⁷ To investigate replacing noble metal catalysts with earth-abundant copper,⁸ we targeted diastereomeric precursors **G** and **G'** (Scheme 2), such as the cations [Cu(diphos*)(PHRR')(L_n)]⁺ (L = 2-electron ligand, n = 0 or 1) or neutral halide complexes Cu(diphos*)(PHRR')(X). To avoid displacement by secondary phosphines, the chiral chelate diphos* should bind tightly to copper; ideally, its sterics, rigidity, and bite angle could be tuned to avoid formation of the unwanted bis(chelate) [Cu(diphos*)₂]⁺. We chose the family of commercially available chiral bis(phospholanes) as electron-rich donors which meet these requirements (see Scheme 3).⁹

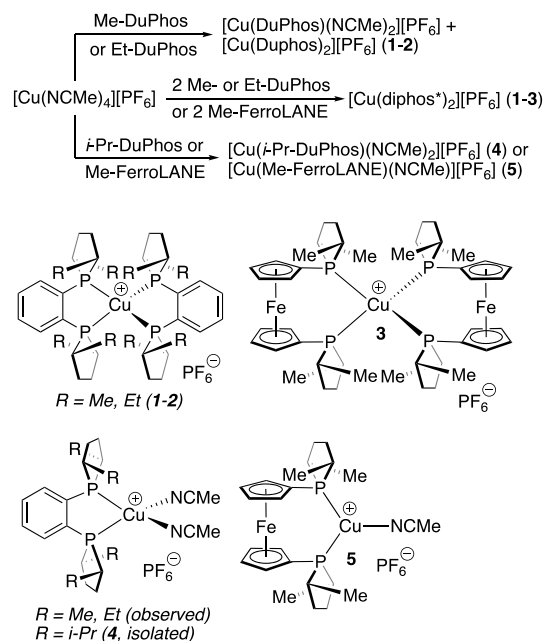
Received: April 30, 2019

Scheme 1. Cu(I) Secondary Phosphine Complexes

Scheme 2. Interconversion of Diastereomeric Cu(diphos*) Secondary Phosphine (G/G') and Phosphido (H/H') Complexes and the Structure of P-Stereogenic Phosphido Complex I, which Contains a Chiral P-Substituent^a

^a[Cu]^{*} = [Cu(diphos*)(L)_n]⁺ or Cu(diphos*)(X); L = two-electron ligand, n = 0 or 1, X = halide.

Diastereomers **G** and **G'** could interconvert by the two-step sequence shown in Scheme 2. After secondary phosphine dissociation and acid- or base-mediated P-epimerization, which occurs under mild conditions, recoordination yields a thermodynamic mixture whose ratio is controlled by the chiral diphos* ligand.¹⁰ Similarly, after base-mediated deprotonation or dehydrohalogenation of **G/G'**, the resulting phosphido complexes **H** and **H'** could interconvert by pyramidal inversion at P.¹¹ Although both processes are well-precedented for other metals, neither one has been observed for copper, for which no chiral secondary phosphine complexes are known. We recently reported the first P-stereogenic Cu-phosphido complex (**I**, Scheme 2), which contained a chiral P-substituent, but we observed only one set of NMR signals for it even at low temperature, suggesting that diastereomer interconversion was still fast on the NMR time scale or that one isomer was formed

Scheme 3. Synthesis of Cationic Cu(diphos*) Complexes 1–5^a

^aAs a consequence of the Cahn–Ingold–Prelog rules, (*R,R*)-Me-DuPhos and (*R,R*)-*i*-Pr-DuPhos, despite the same (*R,R*) label, have opposite absolute configurations.¹⁴ For convenience, only one configuration is shown for *i*-Pr-DuPhos complex **4** and its Me/Et analogues.

preferentially.¹² Here, by studying such diastereoselection in **G/G'** and **H/H'**, we have shown that chiral diphos* ligands can control P-configuration in secondary phosphine or phosphido groups in tetrahedral or trigonal planar complexes, as observed previously in the more commonly examined square planar and octahedral analogues.^{10,11}

RESULTS AND DISCUSSION

Synthesis of Cationic Cu(I)(diphos*) Complexes.

Treatment of [Cu(NCMe)₄][PF₆] with one equivalent of a chiral bis(phospholane) gave either the target [Cu(diphos*)(NCMe)_n][PF₆], the unwanted [Cu(diphos*)₂][PF₆], or both (Scheme 3). The less sterically demanding Me- and Et-DuPhos gave mixtures; the [Cu(DuPhos)₂][PF₆] complexes **1** and **2** were isolated by using two equivalents of ligand. The bulkier *i*-Pr-DuPhos and the larger bite angle Me-FerroLANE gave complexes **4** and **5**, which contained two and one acetonitrile ligands, respectively.¹³ No bis(chelate) was formed with one equivalent of these ligands, but adding a second equivalent gave [Cu(Me-FerroLANE)₂][PF₆] (**3**), which appeared to be in equilibrium with **5** and acetonitrile. However, removing the solvents under vacuum enabled isolation of **3**.

The crystal structure of **1** (Figure 1) showed the expected distorted tetrahedral geometry with an average Me–DuPhos bite angle of 90.61(3)°. The bond lengths and angles at the copper center in **1** (Table S1, Supporting Information) were similar to those in related complexes of the *o*-phenylene-bridged bis(phosphines) dppBz (1,2-bis(diphenylphosphino)benzene)¹⁵ and dppQx (1,2-bis(diphenylphosphino)quinoxaline).¹⁶

Synthesis or Generation of Cationic and Neutral Cu(I)(diphos*) Secondary Phosphine Complexes. These

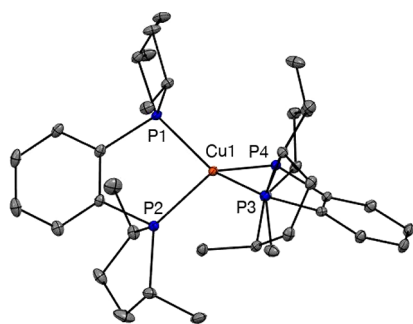
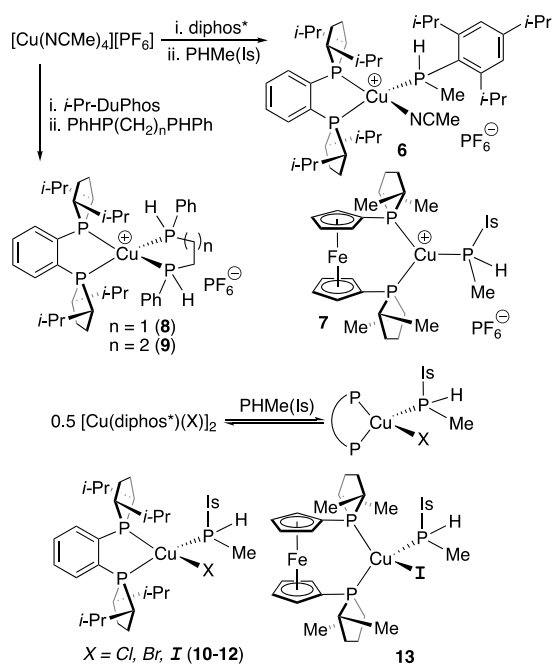


Figure 1. ORTEP diagram of the cation in $[\text{Cu}((R,R)\text{-Me-DuPhos})_2][\text{PF}_6]$ (**1**).

results showed that formation of undesired $[\text{Cu}(\text{diphos}^*)_2]^+$ could be avoided with *i*-Pr-DuPhos and Me-FerroLANE ligands. To prepare secondary phosphine complexes, we chose PHMe(Is) (Is = 2,4,6-*i*-Pr)₃C₆H₂), in which steric differentiation between the P-substituents was intended to promote diastereoselective binding, and the chelates PhHP-(CH₂)_{*n*}PhPh (*n* = 2, 3). Reaction of $[\text{Cu}(\text{NCMe})_4][\text{PF}_6]$ with diphos* and these secondary phosphines gave the isolable cationic complexes $[\text{Cu}((R,R)\text{-}i\text{-Pr-DuPhos})(\text{PHMe}(\text{Is}))(\text{NCMe})][\text{PF}_6]$ (**6**), $[\text{Cu}((R,R)\text{-Me-FerroLANE})(\text{PHMe}(\text{Is}))][\text{PF}_6]$ (**7**), and $[\text{Cu}((R,R)\text{-}i\text{-Pr-DuPhos})(\text{PhHP}(\text{CH}_2)_n\text{PhPh})][\text{PF}_6]$ (**8** and **9**, *n* = 2 or 3, Scheme 4).

Scheme 4. Synthesis and Generation of Cu(diphos*) Secondary Phosphine Complexes



Treatment of the halide-bridged dimers¹⁷ $[\text{Cu}(\text{diphos}^*)(\text{X})]_2$ with PHMe(Is) generated the labile adducts $\text{Cu}(\text{diphos}^*)(\text{PHMe}(\text{Is}))(\text{X})$ (diphos* = *i*-Pr-DuPhos, X = Cl, Br, I (**10–12**); diphos* = (*R,R*)-Me-FerroLANE, X = I (**13**)), which were characterized by NMR spectroscopy.¹⁸ We were not able to isolate pure bulk samples of **10–13** by recrystallization because secondary phosphine coordination was reversible, but small amounts of **10** and **11** were obtained and crystallographically characterized (see below).¹⁹

NMR data (see Table 1, the Experimental Section, and the Supporting Information) showed that the secondary phosphine complexes were formed diastereoselectively, as anticipated. Diastereomer ratios (dr) were small for complexes of PHMe(Is), ranging from 1:1 to 2:1, but for bis(secondary phosphine) complexes **8** and **9**, two of the expected three diastereomers were formed preferentially, with one *C*₂-symmetric isomer disfavored.

Crystal Structures of Secondary Phosphine Complexes 6 and 8–11 and the Computed Structure of 7.

Figures 2–5 show ORTEP diagrams of the secondary phosphine complexes **6** and **8–10**. Crystallographic data are summarized in Table 2 and the Supporting Information, which also includes the structure of disordered **11**. In all cases, the crystals investigated contained only one of the two (or three) diastereomers observed in solution, with *S*- and *R*-enantiomers of PHMe(Is) found in **6** and **10**, respectively (Figures 2 and 5). Crystals of complexes **8** and **9** contained *C*₂-symmetric (*S,S*)-bis(secondary phosphines) (Figures 3 and 4). The bent acetonitrile coordination in **6** (Figure 2, Cu–N–C angle = 159.5(6)°, which has been observed previously,²² is presumably due to steric effects of the large *i*-Pr-DuPhos and isityl groups. Changing from NCMe to Cl in **6** and **10** or increasing the linker length from two to three CH₂ groups in **8** and **9** had little effect on the Cu–P distances or the bond angles in these distorted tetrahedral complexes (Table 2), although the bis(secondary phosphine) bite angle increased from **8** (89.8(1)°) to **9** (95.96(9)°), as expected. Gas-phase DFT calculations on the cation in **7** (see the Supporting Information for details) showed the expected distorted trigonal planar geometry with an average FerroLANE bite angle of 113.96°. The computed energy difference between the two diastereomers (1.8 kcal/mol) was in reasonable agreement with the observed dr (2:1), considering that anion and solvent were not included.

NMR Characterization and Solution Dynamics of Secondary Phosphine Complexes. As in related secondary phosphine complexes,^{2–6} binding to copper resulted in coordination chemical shifts and increases in ¹J_{P_H, which were larger in cations **6–9** than in neutral **10–13** (Table 1). The ³¹P{¹H} NMR signals were broadened by the ⁶³Cu and ⁶⁵Cu quadrupoles,²³ and in some cases from exchange processes, which are described in more detail below. ABX ³¹P{¹H} NMR spin systems with inequivalent diphos* ³¹P nuclei were expected for **6** and **7** and **10–13** because the *C*₂ symmetry of the Cu(diphos*) unit should be broken in these complexes by the presence of the P-stereogenic PHMe(Is) ligand. However, A₂X patterns (apparent *C*₂ symmetry) were observed, presumably because the secondary phosphine was positioned approximately in between the diphos* P-donors in the distorted tetrahedral environment, so the diphos* P nuclei were not well-differentiated. Only broad ³¹P{¹H} NMR signals were observed for the bis(secondary phosphine) complexes **8** and **9**.}

As expected, we observed dynamic processes involving secondary phosphine exchange by ³¹P{¹H} and ¹H NMR spectroscopy. The lability of PHMe(Is) coordination in the halide complexes $\text{Cu}((R,R)\text{-}i\text{-Pr-DuPhos})(\text{PHMe}(\text{Is}))(\text{X})$ (**10–12**) was demonstrated most clearly by a ³¹P{¹H} NMR spectroscopic titration (Figures S8–S12, Supporting Information) in which aliquots of the secondary phosphine were added to $[\text{Cu}((R,R)\text{-}i\text{-Pr-DuPhos})(\text{Br})]_2$ in THF to generate **11** (ca. 0.1 M). Only one set of broad ³¹P NMR DuPhos signals, with

Table 1. $^{31}\text{P}\{^1\text{H}\}$ NMR and Selected ^1H NMR Data for $\text{Cu}(\text{diphos}^*)$ Secondary Phosphine and Phosphido Complexes^a

complex	$^{31}\text{P}\{^1\text{H}\}$ NMR δ (diphos*)	$^{31}\text{P}\{^1\text{H}\}$ NMR δ (PHRR')	$^2J_{\text{PP}}$ (Hz)	$^1J_{\text{PH}}$ (Hz)	^1H NMR δ (PH)	dr
$[\text{Cu}(i\text{-Pr-DuPhos})(\text{PHMe}(\text{Is}))(\text{NCMe})][\text{PF}_6]$ (6) ^b	8.4, 6.5	-87.6, -89.7	65, 75	314, 315	5.64, 5.59	1.3:1
$[\text{Cu}(\text{Me-FerroLANE})(\text{PHMe}(\text{Is}))][\text{PF}_6]$ (7) ^c	11.0	-90.3, -92.9	113, 107	321	5.86	2:1
$\text{Cu}(i\text{-Pr-DuPhos})(\text{PHMe}(\text{Is}))(\text{Cl})$ (10) ^d	3.6	-100.4, -102.2		256, 251	4.81, 4.74	1:1
$\text{Cu}(i\text{-Pr-DuPhos})(\text{PHMe}(\text{Is}))(\text{Br})$ (11) ^d	4.6	-100.5, -102.3		255, 250	4.82, 4.74	1:1
$\text{Cu}(i\text{-Pr-DuPhos})(\text{PHMe}(\text{Is}))(\text{I})$ (12) ^d	3.4	-103.6, -104.9		246, 242	4.74, 4.66	1:1
$\text{Cu}(\text{Me-FerroLANE})(\text{PHMe}(\text{Is}))(\text{I})$ (13) ^d	2.5	-103.9, -104.5		249, 244	4.72, 4.67	1.2:1
$[\text{Cu}(i\text{-Pr-DuPhos})(\text{PhHP}(\text{CH}_2)_2\text{PPh})][\text{PF}_6]$ (8) ^{d,e}	22.8	-29.5		324, 333, 318/304	5.53, 5.43, 5.34/5.23	1:3.3:5
$[\text{Cu}(i\text{-Pr-DuPhos})(\text{PhHP}(\text{CH}_2)_3\text{PPh})][\text{PF}_6]$ (9) ^{d,e}	20.0	-37.7		303, 318, 305	5.44, 5.37, 5.29-5.19	f
$\text{Cu}(i\text{-Pr-DuPhos})(\text{PMeI})$ (14) ^g	7.6, 5.0	-107.2, -109	90, 94			1:4
$\text{Cu}(i\text{-Pr-DuPhos})(\text{PHMe}(\text{Is}))(\text{OSiMe}_3)$ (15) ^{g,h}	3.0 (v. br)	-108.4, -110.1		229, 216		1:1
$\text{Cu}(\text{Me-FerroLANE})(\text{PMeI})$ (17) ⁱ	10.2, 8.8	-94.9, -98.9	114, 110			5:1

^aSee the Experimental Section for $^{31}\text{P}\{^1\text{H}\}$ NMR data for the PF_6 anion. The $^{31}\text{P}\{^1\text{H}\}$ NMR chemical shift standard was 85% H_3PO_4 . Coupling constants are reported in Hz. Coordination chemical shifts can be assessed from data for the free ligands: *i*-Pr-DuPhos: δ -11.2 (C_6D_6);¹⁴ Me-FerroLANE (δ -1.1 (THF)),²⁰ and PHMe(Is) (δ -113.2 (Et_2O), J_{PH} = 214 Hz).²¹ ^1H NMR in CD_2Cl_2 , 25 °C; $^{31}\text{P}\{^1\text{H}\}$ NMR in CD_2Cl_2 at -15 °C. ^c CDCl_3 , 25 °C, 0.01 M for ^{31}P NMR, 0.1 M for ^1H NMR (J_{PH} measurement). ^d CD_2Cl_2 , 25 °C. ^eMixture of three diastereomers (two C_2 -symmetric, one C_1 -symmetric); see the Results and Discussion and Experimental Section for details. ^fNot determined (overlapping peaks). ^gTHF, 25 °C. ^h ^{31}P NMR chemical shifts, especially of the PHMe(Is) group, differed when **15** was generated from precursors **6**, **11**, or **16**. Excess secondary phosphine, which was present from generation of **11** by addition of PHMe(Is) to $[\text{Cu}(i\text{-Pr-DuPhos})(\text{Br})]_2$, appeared to exchange rapidly with **15** on the NMR time scale, as observed for **10**–**12**. ⁱTHF-*d*₈, -35 °C.

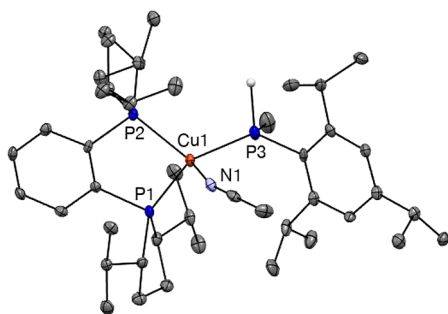


Figure 2. ORTEP diagram of the cation in $[\text{Cu}((R,R)\text{-}i\text{-Pr-DuPhos})((S)\text{-PHMeIs})(\text{NCMe})][\text{PF}_6]$ (**6**). The P–H atom was located and freely refined.

no P–P coupling, was observed throughout the titration, in which this resonance shifted from δ -7.2 in the starting dimer to δ 5.5 with 1.6 equiv of PHMe(Is) to copper. Two broad signals due to coordinated secondary phosphines were observed with shifts varying from -98.2 and -103.8 ppm for the two diastereomers (0.23 equiv of phosphine per Cu) to -107.1 and -109.5 ppm (1.6 equiv of PHMe(Is) per Cu), approaching the chemical shift of the free phosphine in this solvent (-110.0 ppm). Similarly, J_{PH} for these signals decreased from 248 Hz (0.23 equiv of phosphine per Cu) to 226 and 219 Hz (1.6 equiv), approaching the value for the free phosphine (214 Hz). These observations are consistent with rapid exchange on the NMR time scale between the free phosphine and the two diastereomers of **11** (**G** and **G'** in Scheme 2), but slow exchange between these isomers. Similarly, when halide complexes **10**, **12**, and **13** were generated by addition of one or more PHMe(Is) per copper to $[\text{Cu}(\text{diphos}^*)(\text{X})]_2$, $^{31}\text{P}\{^1\text{H}\}$ NMR signals due to two diastereomers **G/G'** in rapid exchange with free secondary phosphine were observed.

Isolation of cations **6** and **7** enabled investigation of related dynamic processes in the absence of free secondary phosphine.

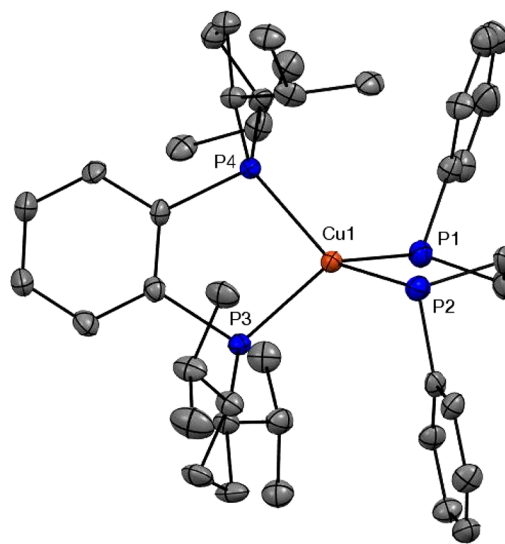


Figure 3. ORTEP diagram of the cation in $[\text{Cu}((R,R)\text{-}i\text{-Pr-DuPhos})((S,S)\text{-PhHP}(\text{CH}_2)_2\text{PPh})][\text{PF}_6] \cdot 0.5\text{Stoluene}$ (**8**, one of the two independent molecules in the unit cell, with solvent and disordered anion omitted).

For DuPhos complex **6** in $\text{C}_2\text{D}_2\text{Cl}_4$, the $^{31}\text{P}\{^1\text{H}\}$ NMR spectrum at room temperature (Figure S1) contained two sets of A_2X signals, consistent with slow exchange between the diastereomers on the NMR time scale, as seen for the neutral analogues **10**–**12**. Even at 105 °C, this exchange remained slow on the NMR time scale, as shown by observation of separate ^1H NMR signals of the two diastereomers. Presumably, although reversible secondary phosphine dissociation was fast, as in Scheme 2, epimerization remained slow. In the $^{31}\text{P}\{^1\text{H}\}$ NMR spectrum (Figure S2), the two DuPhos signals coalesced on heating into a single peak, and the P–P coupling was lost, consistent with rapid PHMe(Is) dissociation. Although two different secondary phosphine $^{31}\text{P}\{^1\text{H}\}$

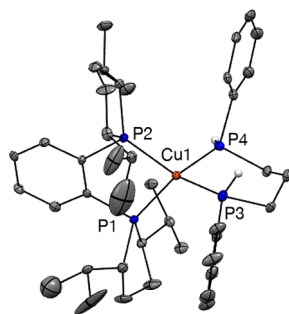


Figure 4. ORTEP diagram of the cation in $[\text{Cu}((R,R)\text{-}i\text{-Pr-DuPhos})((S,S)\text{-PhHP}(\text{CH}_2)_3\text{PHPh})][\text{PF}_6]$ (**9**). The P–H atoms were located and freely refined.

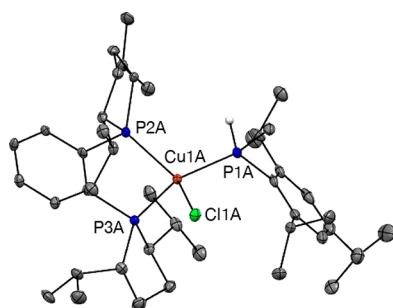


Figure 5. ORTEP diagram of $\text{Cu}((R,R)\text{-}i\text{-Pr-DuPhos})((R)\text{-PHMe(Is)})(\text{Cl})$ (**10**, one of the four independent molecules in the unit cell). The P–H atoms were located and refined with a constraint of a 1.32 Å P–H bond length.

NMR signals would be expected, they also coalesced, which we ascribe to accidental degeneracy of these temperature-dependent chemical shifts. At higher concentration, these reversible spectral changes occurred at lower temperature (Figures S3 and S4), consistent with intermolecular exchange as in Scheme 2. NMR spectra of Me-FerrolANE complex **7** showed similar concentration dependence (Figures S31 and S32). At room temperature, well-resolved $^{31}\text{P}\{^1\text{H}\}$ NMR doublet and triplet signals (apparent A_2X spin system) due to the two diastereomers were observed at 0.01 M in CDCl_3 . At 0.1 M, two $^{31}\text{P}\{^1\text{H}\}$ NMR PHMe(Is) signals were still observed, but they were broader, and no P–P coupling was seen.

Analogous ligand dissociation and intermolecular exchange in chelate complexes **8** and **9** is unlikely, but dynamic processes still affected their NMR spectra. In **8**, most of the ^1H NMR signals at room temperature, including four sharp *i*-Pr methyl doublets, could be assigned to a C_2 -symmetric diastereomer, but the presence of several broad peaks suggested that another isomer, which was undergoing exchange on the NMR time

scale, was present. At -70°C , four ^1H NMR Me doublets for C_2 -**8** plus the expected eight Me doublets for C_1 -**8** were observed (Figures S5–S7). We propose that this process involves dissociation of one arm of the bis(secondary phosphine) in C_1 -**8** to form a three-coordinate intermediate and then reattachment on the opposite side of the metal center (Scheme 5). The ^1H NMR spectrum of **9** was similar, but we did not investigate it in detail because we could not isolate this complex in pure form.

Generation of P-Stereogenic Phosphido Complexes $\text{Cu}(\text{diphos}^*)(\text{PMels})$ (**14** and **17**) by Deprotonation of Cationic Secondary Phosphine Complexes **6** and **7** or Dehydrohalogenation of **11**.

Treatment of *i*-Pr-DuPhos complexes **6** or **11** with NaOSiMe_3 generated the unstable target P-stereogenic phosphido complex **14** as a 4:1 mixture of diastereomers, which was identified by its characteristic doublet (DuPhos) and triplet (PMels) $^{31}\text{P}\{^1\text{H}\}$ NMR signals (Scheme 6, see Table 1 for NMR data and Figures S56 and S57). The $^{31}\text{P}\{^1\text{H}\}$ NMR spectra of these reaction mixtures also contained signals assigned to $\text{Cu}((R,R)\text{-}i\text{-Pr-DuPhos})\text{-}(\text{PHMe(Is)})(\text{OSiMe}_3)$ (**15**) and $[\text{Cu}((R,R)\text{-}i\text{-Pr-DuPhos})\text{-}(\text{OSiMe}_3)]_n$ (**16**); the latter was identified by independent synthesis (Scheme 6).²⁴ When this mixture was formed from **11** which contained excess secondary phosphine, or by addition of PHMe(Is) to **16**, rapid exchange of PHMe(Is) with **15** on the NMR time scale was observed, as for the analogous halide complexes **10**–**12**. These observations were consistent with the equilibria shown in Scheme 6, in which both coordination of PHMe(Is) to $\text{Cu}((R,R)\text{-}i\text{-Pr-DuPhos})\text{-}(\text{OSiMe}_3)$ and proton transfer interconverting **14** and **15** are reversible; we observed similar equilibria involving NHC-ligated $\text{Cu}(\text{IPr})(\text{OSiMe}_3)$ and primary phosphines in the formation of **I** (Scheme 2) and related complexes.¹² They also suggest that coordination of acetonitrile to phosphido complex **14** is either weak and reversible or does not occur at all. Further investigation of this system was hampered by decomposition, which occurred at room temperature to yield *i*-Pr-DuPhos and other unidentified products.

Similarly, treatment of Me-FerrolANE cation **7** with NaOSiMe_3 gave phosphido complex **17** as a 5:1 mixture of diastereomers (Scheme 6, Table 1, Figure S68), along with the decomposition products Me-FerrolANE and PHMe(Is). To further study these unstable complexes, we computed the DFT gas-phase structures (Figure 6) of the two diastereomers of **17**. They differed in energy by 1.1 kcal/mol, consistent with the observed 5:1 ratio, and contained pyramidal Cu-phosphido groups (average angle sum = 316.7°), as expected.

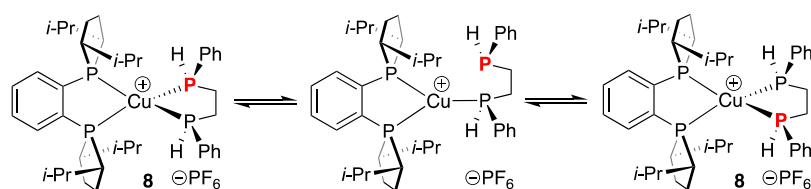
For the diastereomeric phosphido complexes **14** and **17**, the enrichment of one isomer, in a dr which did not match that of the precursor, was consistent with the hypothesized P-

Table 2. Selected Average Bond Lengths (Å) and Angles (deg) for $[\text{Cu}((R,R)\text{-}i\text{-Pr-DuPhos})(\text{PHMe(Is)})(\text{NCMe})][\text{PF}_6]$ (**6**), $\text{Cu}((R,R)\text{-}i\text{-Pr-DuPhos})(\text{PHMe(Is)})(\text{Cl})$ (**10**), $[\text{Cu}((R,R)\text{-}i\text{-Pr-DuPhos})((S,S)\text{-PhHP}(\text{CH}_2)_2\text{PHPh})][\text{PF}_6]\cdot 0.5\text{Stoluene}$ (**8**), and $[\text{Cu}((R,R)\text{-}i\text{-Pr-DuPhos})((S,S)\text{-PhHP}(\text{CH}_2)_3\text{PHPh})][\text{PF}_6]$ (**9**)^a

complex	Cu–P (DuPhos)	Cu–P (phosphine)	P–Cu–P (DuPhos)	X(P)–Cu–P (phosphine) ^b	P–Cu–P'	Cu–X	X–Cu–P (DuPhos)
6	2.280(2)	2.273(2)	90.95(7)	95.30(18)	123.55(9)	2.049(7)	112.6(2)
10	2.264(2)	2.257(2)	90.36(8)	103.04(8)	119.26(8)	2.3075(19)	112.81(9)
8	2.259(3)	2.280(3)	90.9(1)	89.8(1)	119.9(1)		
9	2.298(3)	2.282(3)	90.42(9)	95.96(9)	118.08(9)		

^aAverage values for bond lengths and angles; note there were four independent molecules in **10** and two in **8**. ^bIn **6**, X = NCMe; in **10**, X = Cl. X–Cu–P angles for **6** and **10**, P–Cu–P angles for **8** and **9**

Scheme 5. Proposed Origin of Fluxional Behavior in Cation 8 via Dissociative Interconversion of the Two Donor Sites of the (R,S)-Bis(Secondary Phosphine)



Scheme 6. Generation of Unstable P-Stereogenic Copper-Phosphido Complexes 14 and 17

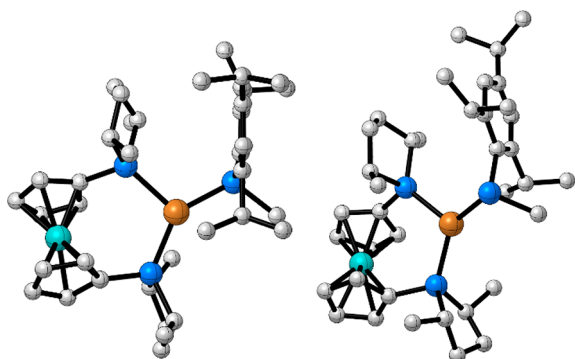
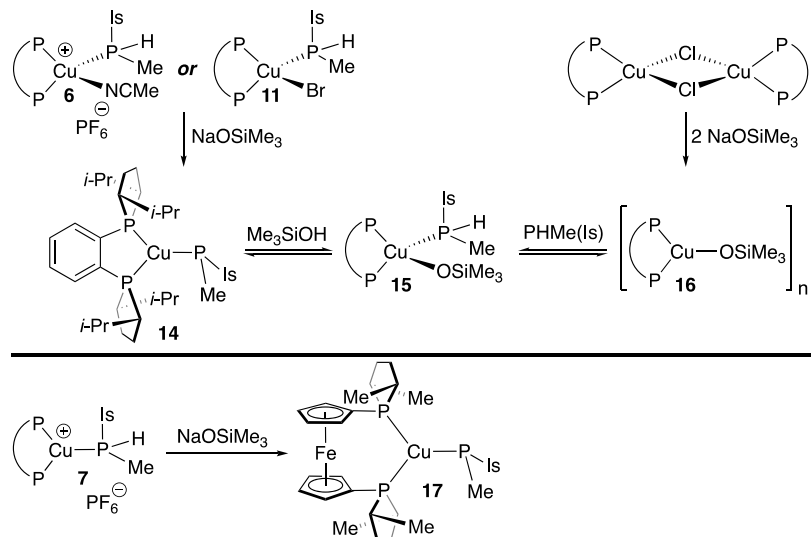


Figure 6. Computed gas-phase (B3LYP-D3/LACV3P/THF/ZPE) DFT structures of the two diastereomers of Cu((R,R)-Me-FerroLANE)(PMeIs) (17).**

inversion process of Scheme 2. However, because these complexes decomposed on warming, we could not observe coalescence of their $^{31}\text{P}\{^1\text{H}\}$ NMR signals or determine activation barriers for pyramidal inversion. Instead, DFT studies of the simplified model complex $\text{Cu}(\text{H}_2\text{PCH}_2\text{CH}_2\text{PH}_2)(\text{PH}_2)$ revealed barriers of 1.4 and 11.4 kcal/mol, respectively, for rotation around the $\text{Cu}-\text{PH}_2$ bond and for inversion of the $\text{Cu}-\text{PH}_2$ group via a planar transition state. These values, which are similar to those observed for phosphido complexes of other metals, are consistent with the experimental observations on 14 and 17.¹¹

CONCLUSIONS

The synthesis and generation of novel diastereomeric cationic and neutral $\text{Cu}(\text{diphos}^*)$ secondary phosphine complexes G/

G' have enabled us to test the hypotheses of Scheme 2. As anticipated, phosphine dissociation from labile $\text{Cu}(\text{I})$ occurred readily. Secondary phosphine epimerization, which presumably resulted in the observed diastereoselection, was slow on the ^1H NMR time scale in cation 6 even at 105 °C in $\text{C}_2\text{D}_2\text{Cl}_4$. Generation of the target P-stereogenic Cu-phosphido complexes as mixtures of diastereomers H/H', whose dr values did not match those of the precursor cations, was consistent with the proposed P-inversion process, as were DFT calculations on a model system, but their instability even at low temperature prevented further characterization of their dynamics. Diastereoselection in formation of secondary phosphine or phosphido complexes G/G' and H/H' was low and did not show simple correlations with coordination number, diphos* bite angle, or other structural parameters. However, this control of phosphido P-configuration in the proposed intermediates $\text{Cu}(\text{diphos}^*)(\text{PRR}')$ is potentially useful in catalytic asymmetric reactions, which are now under investigation.

EXPERIMENTAL SECTION

Unless otherwise noted, all reactions and manipulations were performed in dry glassware under a nitrogen atmosphere at 20 °C in a drybox or using standard Schlenk techniques. Pentane, CH_2Cl_2 , ether, THF, and toluene were dried over alumina columns similar to those described by Grubbs.²⁵ NMR spectra were recorded using 500 or 600 MHz spectrometers. ^1H or ^{13}C NMR chemical shifts are reported vs Me_4Si and were determined by reference to the residual ^1H or ^{13}C solvent peaks. ^{31}P NMR chemical shifts are reported vs H_3PO_4 (85%) used as an external reference. Coupling constants are reported in Hz as absolute values unless noted otherwise. Unless indicated, peaks in NMR spectra are singlets. Elemental analyses were provided by Quantitative Technologies Incorporated/Intertek Pharmaceutical Services (Whitehouse, NJ) or Atlantic Microlab

(Norcross, GA). Mass spectra were recorded at the University of Illinois Urbana–Champaign (<https://scs.illinois.edu/resources/cores-sc-service-facilities/massspectrometry-lab>). Reagents were from commercial suppliers or prepared by the literature methods: $[\text{Cu}(\text{NCMe})_4][\text{PF}_6]$,²⁶ $\text{PHMe}(\text{Is})$,²¹ and $[\text{Cu}(\text{diphos}^*)(\text{X})_n]$ (diphos* = (R,R) -*i*-Pr-DuPhos, X = Cl, Br, I; diphos* = (R,R) -Me-FerroLANE, X = I).¹⁷

[Cu((*R,R*)-Me-DuPhos)₂][PF₆] (1). A slurry of $[\text{Cu}(\text{NCMe})_4][\text{PF}_6]$ (61 mg, 0.16 mmol) in 1 mL of THF was treated with a solution of (R,R) -Me-DuPhos (50 mg, 0.16 mmol) in 3 mL of THF. Upon stirring, the mixture became homogeneous and clear. The ³¹P NMR spectrum showed two peaks (δ 31.8 and 9.3), presumably $[\text{Cu}(\text{Me-DuPhos})_2][\text{PF}_6]$ and $[\text{Cu}(\text{Me-DuPhos})(\text{NCMe})_2][\text{PF}_6]$. Addition of a second equivalent of (R,R) -Me-DuPhos (50 mg, 0.16 mmol) in 2 mL of THF resulted in precipitation of a white solid. The ³¹P NMR spectrum of this mixture contained only one peak at 32.3 ppm. The solution was pumped down under vacuum. The residue was dissolved in 3 mL of methylene chloride, and the solution was filtered through Celite. The filtrate was layered with 15 mL of pentane and cooled to -30 °C, giving a white solid (100 mg, 0.121 mmol, 75%). X-ray quality crystals were grown by vapor diffusion of Et₂O into a concentrated solution of CH₂Cl₂ at -30 °C.

Anal. Calcd for C₃₆H₅₆CuF₆P₅: C, 52.65; H, 6.87. Found: C, 52.04; H, 6.87. HRMS *m/z* calcd for C₃₆H₅₆P₄Cu (M⁺): 675.2629. Found: 675.2651. ³¹P{¹H} NMR (CD₂Cl₂): δ 32.0 (broad), -143.6 (septet, *J* = 711). ¹H NMR (CD₂Cl₂): δ 7.70–7.67 (m, 4H, Ar), 7.60–7.58 (m, 4H, Ar), 2.74–2.72 (m, 4H, CH), 2.46–2.38 (overlapping m, 8H, CH and CH₂), 2.20–2.19 (m, 4H, CH₂), 1.87–1.79 (m, 4H, CH₂), 1.60–1.52 (m, 4H, CH₂), 1.21–1.16 (m, 12H, CH₃), 0.89–0.83 (m, 12H, CH₃). ¹³C{¹H} NMR (CD₂Cl₂): δ 142.2–141.8 (m, Ar), 133.2–133.1 (m, Ar), 130.4 (Ar), 38.0 (quintet, *J* = 6, CH), 37.7 (quintet, *J* = 6, CH), 36.5 (m, CH₂), 36.5–36.4 (m, CH₂), 20.2 (quintet, *J* = 6, CH₃), 15.3 (m, CH₃). UV–vis (CH₂Cl₂, 1×10^{-5} M): λ_{max} = 426 and 722 nm.

[Cu((*R,R*)-Et-DuPhos)₂][PF₆] (2). A slurry of $[\text{Cu}(\text{NCMe})_4][\text{PF}_6]$ (85 mg, 0.24 mmol) in 2 mL of THF was treated with a solution of (R,R) -Et-DuPhos (86 mg, 0.24 mmol) in 2 mL of THF; stirring gave a clear, homogeneous solution with two ³¹P NMR signals (δ 31.0 and 5.3), presumably due to $[\text{Cu}(\text{Et-DuPhos})_2][\text{PF}_6]$ and $[\text{Cu}(\text{Et-DuPhos})(\text{NCMe})_2][\text{PF}_6]$. A second equivalent of (R,R) -Et-DuPhos (86 mg, 0.24 mmol) in 2 mL of THF was added. The ³¹P NMR spectrum of this mixture contained the same two peaks at 31.0 and 5.3 ppm, though the peak at 5.3 ppm was smaller. Upon addition of a third portion of (R,R) -Et-DuPhos (7.8 mg, 0.021 mmol), the ³¹P NMR spectrum contained only one peak at 30.9 ppm. The solution was concentrated under reduced pressure. The residue was dissolved in 3 mL of methylene chloride and filtered through Celite. The filtrate was layered with 15 mL of pentane and cooled to -30 °C, giving a white solid (130 mg, 0.165 mmol, 70%).

HRMS *m/z* calcd for C₄₄H₇₂CuP₄ (M⁺): 787.3881. Found: 787.3880. ³¹P{¹H} NMR (CD₂Cl₂): δ 30.9 (broad), -143.6 (septet, *J* = 711). ¹H NMR (CD₂Cl₂): δ 7.68–7.62 (m, 4H, Ar), 7.58–7.54 (m, 4H, Ar), 2.52–2.36 (m, 8H, CH), 2.32–2.20 (m, 4H, CH₂), 2.12–2.00 (m, 4H, CH₂), 1.86–1.74 (m, 4H, CH₂), 1.60–1.48 (m, 8H, CH₂), 1.30–1.24 (m, 4H), 1.10–0.88 (m, 32H, CH₃ + CH₂). ¹³C{¹H} NMR (CD₂Cl₂): δ 142.6–142.0 (m, Ar), 132.9 (Ar), 130.3 (Ar), 44.9 (quintet, *J* = 6, CH), 44.7 (quintet, *J* = 6, CH), 32.8 (CH₂), 32.4 (CH₂), 28.5 (quintet, *J* = 6, CH₃).

[Cu((*R,R*)-Me-FerroLANE)₂][PF₆] (3). To a slurry of $[\text{Cu}(\text{NCMe})_4][\text{PF}_6]$ (22 mg, 0.088 mmol) in 1 mL of THF was added a solution of (R,R) -Me-FerroLANE (70 mg, 0.18 mmol, 2 equiv) in 2 mL of THF. The resulting solution was stirred for 10 min and then concentrated under vacuum to give an orange solid (71 mg, 72% yield).

³¹P{¹H} NMR (THF, 25 °C): δ -0.1 (Me-FerroLANE), -142.5 (sp, *J* = 711, PF₆). ¹H NMR (CD₂Cl₂, 25 °C): δ 4.46–4.42 (br m, 8H, Cp CH), 4.33 (4H, Cp CH), 4.13 (4H, Cp CH), 2.70 (4H, CH), 2.30 (4H, CH), 2.03–1.94 (m, 8H, CH₂), 1.46 (12H, Me), 1.40–1.30 (m, 8H, CH₂), 0.79 (12H, Me). ¹³C{¹H} NMR (THF, 25 °C): δ 77.1 (Cp CH), 75.1 (br, quat Cp), 71.8 (Cp CH), 71.1 (Cp CH),

70.5 (Cp CH), 37.0 (CH₂), 36.7 (CH₂), 36.1 (CH), 35.3 (CH), 21.4 (Me), 14.5 (Me). All of the signals were broad.

[Cu((*R,R*)-*i*-Pr-DuPhos)(NCMe)₂][PF₆] (4). A slurry of $[\text{Cu}(\text{NCMe})_4][\text{PF}_6]$ (445 mg, 1.20 mmol) in 3 mL of THF was treated with a solution of (R,R) -*i*-Pr-DuPhos (300 mg, 1.20 mmol) in 4 mL of THF. After being stirred for 1 h, the resulting solution was concentrated under reduced pressure. The residue was washed with pentane and dissolved in 3 mL of methylene chloride. Copper-colored particles were removed by filtration. The filtrate was layered with 15 mL of pentane and cooled to -30 °C, yielding a reddish white solid (603 mg, 0.850 mmol, 71%). This complex decomposed in solution at room temperature, and we could not obtain analytically pure material.

HRMS *m/z* calcd for C₂₈H₄₇NCuP₂ (M–NCMe)⁺: 522.2480. Found: 522.2480. ³¹P{¹H} NMR (CD₂Cl₂): δ 0.4, -143.5 (septet, *J* = 714). ¹H NMR (CD₂Cl₂): δ 7.76–7.74 (m, 2H, Ar), 7.56–7.54 (m, 2H, Ar), 2.66–2.56 (m, 2H), 2.40–2.20 (overlapping m, 4H), 2.24 (6H), 2.10–1.96 (m, 2H), 1.90–1.78 (m, 2H), 1.72–1.60 (m, 2H), 1.27–1.25 (m, 2H), 1.09 (d, *J* = 7, 6H), 0.96 (d, *J* = 7, 6H), 0.95–0.90 (br m, 2H), 0.83 (d, *J* = 7, 6H), 0.65 (d, *J* = 7, 6H). ¹³C{¹H} NMR (CD₂Cl₂): δ 142.6–142.1 (m, Ar), 135.0–134.9 (m, Ar), 130.4 (Ar), 118.8 (br, NCMe), 51.7 (overlapping m), 32.9, 30.5, 28.8, 27.9, 24.6 (m), 23.3 (m), 21.3 (m), 19.0 (m), 2.5 (NCMe).

[Cu((*R,R*)-Me-FerroLANE)(NCMe)₂][PF₆] (5). To a slurry of $[\text{Cu}(\text{NCMe})_4][\text{PF}_6]$ (16 mg, 0.044 mmol) in 1 mL of THF was added a solution of (R,R) -Me-FerroLANE (18 mg, 0.044 mmol) in 1 mL of THF. The resulting orange solution was stirred for 20 min and then concentrated under vacuum to give an orange solid (26 mg, 83% yield). This complex could be recrystallized from THF/pentane.

HRMS *m/z* calcd for C₂₂H₃₂CuP₂Fe (M–NCMe)⁺: 477.0625. Found: 477.0621. ³¹P{¹H} NMR (CDCl₃, 25 °C): δ 9.5 (FerroLANE), -142.9 (sp, *J*_{P–F} = 712, PF₆). ¹H NMR (CDCl₃, 25 °C): δ 4.57 (4H, Cp CH), 4.47 (2H, Cp CH), 4.18 (2H, Cp CH), 2.68 (2H, CH), 2.30 (5H, overlapping CH (2H) and NCMe (3H)), 2.22 (2H, br m, CH₂), 1.99 (2H, CH₂), 1.52 (6H, Me), 1.40 (2H, CH₂), 1.33 (2H, CH₂), 0.82 (6H, Me). ¹³C{¹H} NMR (CDCl₃, 25 °C): δ 118.4 (very br, quat NCMe), 77.2 (overlapping CDCl₃ signal, Cp CH), 72.7 (Cp CH), 71.9 (Cp CH), 71.7–71.5 (m, quat Cp), 71.3 (Cp CH), 36.0 (CH₂), 35.8 (CH), 35.6 (CH₂), 34.3 (CH), 20.9 (Me), 14.0 (Me), 2.4 (NCMe). Note: the 118.4 nitrile signal was initially sharp but became very broad after recrystallization, suggesting fast exchange on the NMR time scale between free and coordinated acetonitrile.

[Cu((*R,R*)-*i*-Pr-DuPhos)(PHMeIs)(NCMe)₂][PF₆] (6). To a slurry of $[\text{Cu}(\text{NCMe})_4][\text{PF}_6]$ (85 mg, 0.23 mmol) in 5 mL of ether was added a solution of (R,R) -*i*-Pr-DuPhos (96 mg, 0.23 mmol) in 2 mL of ether, and the resulting milky-white slurry was stirred for 20 min. A solution of PHMeIs (61.5 mg, 0.23 mmol) in 2 mL of ether was added, and the resulting slurry was stirred for 10 min. After 1 d at -20 °C, the ether was decanted, and the remaining white solid was dried under vacuum (149 mg, 0.16 mmol, 70% yield). X-ray quality crystals were obtained by recrystallization from ether at -20 °C. From ¹H NMR integration, **6** was a 1:1.3 mixture of diastereomers A and B; individual signals due to these isomers were observed for the P–Is, P–H, and P–Me resonances but not for the DuPhos or MeCN ones.

Anal. Calcd for C₄₄H₇₄CuF₆NP₄: C, 57.54; H, 8.12; N, 1.52. Found: C, 58.35; H, 8.25; N, 1.30. MS *m/z* 731.4 (M–NCMe)⁺, 522.2 (M–PHMeIs)⁺, 481.2 (Cu((*i*-Pr-DuPhos))⁺. ³¹P{¹H} NMR (CD₂Cl₂, 25 °C): δ 5.6 (br m, *i*-Pr-DuPhos), -89.8 to -90.7 (br m, PHMeIs), -145 (sp, *J*_{P–F} = 709, PF₆). ³¹P{¹H} NMR (C₂D₂Cl₄, 25 °C): δ 6.0 (d, *J* = 85, *i*-Pr-DuPhos), 4.9 (d, *J* = 86, *i*-Pr-DuPhos), -90 (t, *J* = 85, PHMeIs), -90.6 (t, *J* = 86, PHMeIs), -143 (sp, *J* = 714, PF₆). ³¹P{¹H} NMR (C₂D₂Cl₄, 105 °C): δ 4.9 (*i*-Pr-DuPhos), -90.5 (PHMeIs), -143 (sp, *J* = 723, PF₆). ¹H NMR (CD₂Cl₂, 25 °C): δ 7.73–7.70 (m, 2H, DuPhos Ar), 7.53–7.51 (m, 2H, DuPhos Ar), 7.06 (d, *J* = 2, 2H, Is Ar A), 7.04 (d, *J* = 3, 2H, Is Ar B), 5.64 (br dq, *J* = 314, 6, 1H, PH A), 5.59 (dq, *J* = 315, 6, 1H, PH B), 2.85–2.80 (m, 1H, CH), 2.56–2.50 (m, 2H, DuPhos CH), 2.34–2.28 (m, 2H, CH₂), 2.26–2.20 (m, 2H, CH₂), 2.02–1.96 (m, 2H, DuPhos CH), 1.87 (3H, NCMe), 1.83–1.75 (m, 4H, CH), 1.60–1.58 (br t, *J* = 6, 3H, P–Me B), 1.55–1.53 (br t, *J* = 6, 3H, P–Me A), 1.52–1.47 (m,

2H, CH₂), 1.27 (t, *J* = 6, 6H, Is Me), 1.21–1.20 (br m, 6H, Is Me), 1.17–1.16 (m, 6H, Is Me), 0.84 (d, *J* = 7, 6H, DuPhos *i*-Pr Me), 0.78 (d, *J* = 7, 6H, DuPhos *i*-Pr Me), 0.64 (d, *J* = 7, 6H, DuPhos *i*-Pr Me), 0.57 (d, *J* = 7, 6H, DuPhos *i*-Pr Me). ¹³C{¹H} NMR (CD₂Cl₂, 25 °C): δ 152.5 (quat Is), 152.3 (quat Is), 152.1 (t, *J* = 9, quat Is), 142.0 (t, *J* = 24, quat DuPhos Ar), 135.6 (t, *J* = 3, DuPhos Ar CH), 131.4 (DuPhos Ar CH), 124.0 (m, ipso quat Is), 123.0 (t, *J* = 6, Is CH), 118.9 (br, quat NCMe), 53.0 (t, *J* = 9, DuPhos CH), 52.5 (t, *J* = 9, DuPhos CH), 35.1 (d, *J* = 2, CH), 33.9 (d, *J* = 12, CH), 32.8 (CH₂), 32.0 (t, *J* = 8, CH), 29.6 (CH₂), 29.2 (CH), 25.42 (Me), 25.39 (Me), 25.23 (Me), 25.19 (Me), 24.9 (Me), 24.4 (t, *J* = 5, Me), 24.1 (m, Me), 21.2 (br, Me), 20.2 (t, *J* = 5, Me), 10.6 (d, *J* = 21, P-Me), 9.8 (d, *J* = 20, P-Me), 2.1 (NCMe).

[Cu(*R,R*)-Me-FerroLANE](PHMe(Is))][PF₆] (7). To a slurry of [Cu(NCMe)₄][PF₆] (85 mg, 0.23 mmol) in 2 mL of THF was added a solution of (*R,R*)-Me-FerroLANE (95 mg, 0.23 mmol) in 2 mL of THF, and the resulting orange solution was stirred for 20 min. A solution of PHMe(Is) (58 mg, 0.23 mmol) in 2 mL of THF was added, and the resulting solution was stirred for 10 min, filtered through Celite, and concentrated under vacuum to give an orange powder (149 mg, 92%). This material was a mixture of diastereomers A and B (~2:1) from ³¹P{¹H} and ¹H NMR integration, but only one set each of ¹H and ¹³C NMR signals was observed at room temperature, except for the PH resonances. The NMR spectra were concentration-dependent, presumably due to faster intermolecular exchange at higher concentrations.

HRMS *m/z* calcd for C₃₈H₅₉P₃FeCu(M⁺): 727.2475. Found: 727.2474. ³¹P{¹H} NMR (CDCl₃, 25 °C, 0.1 M): δ 10.6 (FerroLANE), -90.5 (PHMe(Is)), -93.1 (PHMe(Is)), -142.8 (septet, *J*_{P-F} = 713, PF₆). ³¹P{¹H} NMR (CDCl₃, 25 °C, 0.01 M): δ 11.0 (d, *J* = 113, FerroLANE), -90.3 (t, *J* = 113, PHMe(Is)), -92.9 (t, *J* = 107, PHMe(Is)), -142.8 (septet, *J*_{P-F} = 713, PF₆). ¹H NMR (CDCl₃, 25 °C, 0.1 M): δ 7.09 (2H, Is Ar), 5.86 (br dm, *J* = 321, 1H, P-H), 4.68 (2H, Cp), 4.43 (2H, Cp), 4.28 (2H, Cp), 4.24 (2H, Cp), 3.36 (2H, CH), 2.89–2.87 (m, 4H, CH), 2.34–2.31 (br m, 3H, CH and CH₂), 1.93 (3H, CH), 1.49 (very broad, 7H, Me), 1.34–1.23 (overlapping signals, 30H, Is and phospholane Me, plus 2H CH₂), 0.88–0.86 (3H, Me). All signals were broad. ¹³C{¹H} NMR (CDCl₃, 25 °C, 0.1 M): δ 151.9 (quat Is), 151.4 (br m, quat Is), 151.3 (br m, quat Is), 122.4–122.3 (br m, Is Ar CH), 76.1 (t, *J* = 11, Cp CH), 74.6 (Cp CH), 72.0 (Cp CH), 71.7 (Cp CH), 70.6 (br, quat Cp), 36.0 (t, *J* = 13, CH), 35.7 (CH₂), 35.6 (CH₂), 34.3–34.0 (br m, CH), 33.9 (CH), 25.3 (Me), 24.8 (Me), 23.9 (Me), 23.8 (Me), 21.4 (t, *J* = 9, Me), 14.8 (Me). The P-Is quaternary aryl signal was not observed. ¹H NMR (THF-*d*₈, 25 °C, 0.01 M): δ 7.19 (br d, *J* = 3, 2H, Is Ar), 6.06–6.01 (overlapping br dq, 1H, *J*_{P-HA} = 329, 7; *J*_{P-HB} = 330, 6), 4.72 (2H, Cp), 4.47 (2H, Cp), 4.46 (overlapping, 2H, Cp), 4.39 (2H, Cp), 3.51–3.49 (br m, 2H, CH), 3.00 (br m, 3H, CH), 2.93–2.89 (m, 1H, CH), 2.31 (br m, 3H, CH and CH₂), 2.15 (br, 2H), 1.93 (br m, 3H, CH₂), 1.51 (8H), 1.38 (d, 9H, *J* = 7, Me and CH₂), 1.34–1.32 (overlapping d, 9H, Me and CH₂), 1.26–1.24 (overlapping d, *J* = 7, 7, 7H, Me), 0.89–0.87 (3H, Me).

[Cu(*R,R*)-*i*-Pr-DuPhos](PhHP(CH₂)₂PhPh)][PF₆] (8). To a slurry of [Cu(NCMe)₄][PF₆] (85 mg, 0.23 mmol) in 5 mL of ether was added a solution of (*R,R*)-*i*-Pr-DuPhos (117 mg, 0.28 mmol, 1.2 equiv) in 2 mL of ether, and the resulting slurry was stirred for 20 min. A solution of PhHP(CH₂)₂PhPh (80 mg, 0.32 mmol, 1.4 equiv) in 2 mL of ether was added, and the resulting slurry was stirred for 10 min. The ether was decanted, and the white solid was washed (3 × 2 mL) with fresh ether before being dried under vacuum to yield a white solid (169 mg, 84%). The fluxional behavior of the C₁ isomer at room temperature made spectral assignments difficult, with several broad ¹H NMR signals. From the PH region of the ¹H NMR spectrum, there appeared to be three isomers, two C₂ and one C₁, in a ratio of approximately 1(C₂):3.3(C₂):5(C₁). However, most of the other well-resolved ¹H NMR signals at room temperature could be assigned to the major C₂ isomer. Similarly, most of the well-resolved ¹³C{¹H} NMR signals at room temperature could be assigned to the major C₂ isomer, but several broad peaks and a few sharp ones, especially in the aryl region, are presumably due to the other isomers.

At -70 °C, from integration of the ¹H NMR Me signals, the C₂:C₁ ratio was ca. 1.3:1.

HRMS *m/z* calcd for C₄₀H₆₀P₄Cu (M⁺): 727.2942. Found: *m/z* 727.2941. ³¹P{¹H} NMR (CD₂Cl₂, 25 °C): δ 22.8 (br, DuPhos), -29.5 (br, PhHP(CH₂)₂PhPh), -145 (septet, *J* = 710, PF₆). ¹H NMR (CD₂Cl₂, 25 °C): δ 7.70–7.65 (m, 3H), 7.56–7.45 (m, 11H), 5.53 (br d, *J* = 324, C₂' PH), 5.43 (br dm, *J* = 333, C₂ PH), 5.34 (br ddm, *J* = 318, 24, C₁ PH), 5.23 (d of apparent sextets, *J* = 304, 8, C₁ PH), 2.78–2.66 (m, 1H), 2.59–2.52 (septet, *J* = 6, 2H, DuPhos CH), 2.52–2.40 (m, 2H, CH₂), 2.37–2.23 (m, 5H (2H CH₂, 1H *i*-Pr CH, 2H DuPhos CH₂)), 2.16–2.08 (m, 3H, *i*-Pr CH), 1.94–1.87 (m, 2H, DuPhos CH₂), 1.67–1.60 (qd, *J* = 13, 6, 2H, DuPhos CH₂), 1.52–1.45 (qd, *J* = 6, 13, 2H, DuPhos CH₂), 1.29–1.23 (m, 2H, DuPhos CH), 1.19 (d, *J* = 7, 6H, C₂ Me), 1.06–1.02 (br), 1.03 (d, *J* = 7, 6H, C₂ *i*-Pr Me), 1.0–0.7 (very br), 0.38 (br), 0.25 (d, *J* = 7, 6H, C₂ *i*-Pr Me), 0.15 (d, *J* = 7, 6H, C₂ *i*-Pr Me). ¹³C{¹H} NMR (CD₂Cl₂, 25 °C): δ 142.0 (tt, *J* = 25, 4, quat DuPhos), 134.6 (br), 134.3 (t, *J* = 4, Ar CH), 132.9 (d, *J* = 11, Ar CH), 132.1 (t, *J* = 6, Ar CH), 131.7 (d, *J* = 11, Ar CH), 131.0–130.7 (m, quat Ar), 130.9 (Ar CH), 130.5 (Ar CH), 130.4–130.3 (br, Ar CH), 130.3 (Ar CH), 130.1 (Ar CH), 129.6–129.5 (m, Ar CH), 129.3 (d, *J* = 8, Ar CH), 53.0–52.0 (br), 52.0–50.0 (br), 51.7 (t, *J* = 9, DuPhos CH), 49.8 (t, *J* = 9, DuPhos CH), 32.8 (very br), 31.6 (DuPhos CH₂), 31.4 (t, *J* = 8, *i*-Pr CH), 28.8 (DuPhos CH₂), 28.4 (*i*-Pr CH), 23.8 (t, *J* = 4, Me), 23.6–23.3 (m, CH₂, C₁ isomer), 23.5 (br m, Me), 23.1 (tt, *J* = 19, 4, CH₂), 21.8–21.5 (m, CH₂, C₁ isomer), 21.0–20.4 (br), 20.3 (t, *J* = 3, Me), 19.9 (br m, Me), 19.0 (very broad).

³¹P{¹H} NMR (CD₂Cl₂, -70 °C): δ 23.3 (br, DuPhos), 19.4 (br, DuPhos), -28.5 to -33.2 (br, PhHP(CH₂)₂PhPh), -144.8 (septet, *J* = 713, PF₆). ¹H NMR (CD₂Cl₂, -70 °C, selected data): δ 5.48 (br d, *J* = 319, C₂' PH), 5.38 (br d, *J* = 340, C₂ PH), 5.31 (br dd, *J* = 318, 25, C₁ PH), 5.06 (br dm, *J* = 312, C₁ PH), 1.19 (d, *J* = 6, 6H, C₂ Me), 1.02 (d, *J* = 6, 3H, C₁ Me), 0.96 (d, *J* = 6, 6H, C₂ Me), 0.92 (m, 6H, 2 C₁ Me), 0.64 (d, *J* = 6, 3H, C₁ Me), 0.30 (d, *J* = 6, 3H, C₁ Me), 0.19 (d, *J* = 6, 3H, C₁ Me), 0.14 (d, *J* = 6, 6H, C₂ Me), 0.082 (d, *J* = 6, 6H, C₂ Me), 0.038 (d, *J* = 6, 3H, C₁ Me), -0.16 (d, *J* = 6, 3H, C₁ Me).

[Cu(*R,R*)-*i*-Pr-DuPhos](PhHP(CH₂)₃PhPh)][PF₆] (9). To a slurry of [Cu(NCMe)₄][PF₆] (85 mg, 0.23 mmol) in 5 mL of CH₂Cl₂ was added a solution of (*R,R*)-*i*-Pr-DuPhos (117 mg, 0.28 mmol, 1.2 equiv) in 2 mL of CH₂Cl₂, and the resulting solution was stirred for 20 min. A solution of PhHP(CH₂)₃PhPh (82 mg, 0.32 mmol, 1.4 equiv) in 2 mL of CH₂Cl₂ was added, and the resulting solution was stirred for 10 min, filtered through Celite, and placed under vacuum to give a white solid (224 mg, 110%). The solid was washed with ether and pentane in an attempt to remove impurities, but they were not soluble. The ether extract was stored at -20 °C, and after 2 weeks, long, X-ray quality white needles had formed.

HRMS *m/z* calcd for C₄₁H₆₂P₄Cu (M⁺): 741.3098. Found: *m/z* 741.3094. ³¹P{¹H} NMR (CD₂Cl₂, 25 °C): δ 20.0 (br m, *i*-Pr-DuPhos), -37.7 (br m, PhHP(CH₂)₃PhPh), -145 (sp, *J*_{P-F} = 711, PF₆). ¹H NMR (CDCl₃, 25 °C): δ 7.85–7.80 (m, 3H), 7.65–7.25 (br m, 11H), 5.44 (br d, *J* = 303, 2H, C₂' PH), 5.37 (br dm, *J* = 318, 5, 2H, C₂ PH), 5.29–5.19 (br dm, *J* ~ 305, 2H, C₁ PH), 2.48–2.41 (br m, 4H), 2.35–2.30 (br m, 6H), 2.10–2.02 (br m, 6H), 1.65–1.61 (br m, 4H), 1.52 (br, 2H), 1.24 (d, *J* = 7, 6H, Me), 1.07–1.01 (br m), 0.94–0.84 (br m), 0.87 (d, *J* = 7, 6H, Me), 0.72–0.68 (br m), 0.42–0.38 (br m), 0.26 (d, *J* = 7, 6H, Me), -0.01 (d, *J* = 7, 6H, Me). ¹³C{¹H} NMR (CDCl₃, 25 °C): δ 142.0 (tt, *J* = 25, 4, quat DuPhos), 135.0–134.6 (br m), 134.5 (Ar CH), 134.4 (Ar CH), 134.3 (t, *J* = 4, Ar CH), 133.2 (br), 133.0 (t, *J* = 5, Ar CH), 132.6 (d, *J* = 10, Ar CH), 131.7 (m, Ar CH), 131.5 (Ar CH), 131.4 (m, Ar CH), 130.9 (Ar CH), 130.6 (d, *J* = 20, Ar CH), 130.5 (d, *J* = 21, Ar CH), 129.7 (m, Ar CH), 129.4 (d, *J* = 8, Ar CH), 53.5–52.7 (br), 52.3 (t, *J* = 9, DuPhos CH), 50.6–50.4 (br m), 50.2 (t, *J* = 9, DuPhos CH), 33.0–32.0 (very br), 32.0 (DuPhos CH₂), 31.8 (t, *J* = 8, *i*-Pr CH), 29.0 (DuPhos CH₂), 28.8 (*i*-Pr CH), 25.5 (br m, CH₂), 25.0–24.9 (br m, minor CH₂), 24.6 (t, *J* = 4, Me), 24.5–24.2 (br), 23.1, 20.9 (CH₂), 20.8 (t, *J* = 3, Me), 20.7 (t, *J* = 3, Me), 19.4 (br, Me). Note: in contrast to 8, peak overlap in the PH region precluded determination

of the isomer ratio. Because this complex was not obtained in pure form, we did not investigate its variable temperature NMR behavior.

$^{31}\text{P}\{^1\text{H}\}$ NMR Titration of $[\text{Cu}((R,R)\text{-}i\text{-Pr-DuPhos})(\text{Br})]_2$ with PHMe(Is) in THF. $[\text{Cu}((R,R)\text{-}i\text{-Pr-DuPhos})(\text{Br})]_2$ was prepared as reported from CuBr and *i*-Pr-DuPhos and freshly recrystallized from THF/ether at $-30\text{ }^\circ\text{C}$ to give yellow-green crystals.¹⁷ To a solution of this material (79 mg, 0.071 mmol) in 1 mL of THF was added 0.2 mL aliquots (0.032 mmol, 0.23 equiv per Cu) of a stock solution of PHMe(Is) (40 mg, 0.16 mmol, 1.1 equiv per Cu) in 1 mL of THF. After addition was complete, more PHMe(Is) was added as a neat liquid. The reaction was monitored by $^{31}\text{P}\{^1\text{H}\}$ NMR spectroscopy. For details of the resulting spectra, see the Supporting Information.

Generation of $\text{Cu}((R,R)\text{-}i\text{-Pr-DuPhos})(\text{PHMe(Is)})(\text{X})$ (10–12) for NMR Characterization. The dimers $[\text{Cu}((R,R)\text{-}i\text{-Pr-DuPhos})(\text{X})]_2$ were prepared on the 0.14 mmol scale from CuX and *i*-Pr-DuPhos and freshly recrystallized from THF/ether at $-30\text{ }^\circ\text{C}$.¹⁷ NMR samples were prepared in CD_2Cl_2 by addition of PHMe(Is) (35 mg, 0.14 mmol); integration of the DuPhos and secondary phosphine signals showed that a slight excess of PHMe(Is) was present.

NMR Data for $\text{Cu}((R,R)\text{-}i\text{-Pr-DuPhos})(\text{PHMe(Is)})(\text{Cl})$ (10). $^{31}\text{P}\{^1\text{H}\}$ NMR (CD_2Cl_2): δ 3.6 (br, DuPhos), -100.4 (br, PHMe(Is) A), -102.2 (br, PHMe(Is) B), about 1:1 ratio. ^{31}P NMR (CD_2Cl_2): δ 3.7 (br, DuPhos), -100.4 (d, $J = 255$, PHMe(Is) A), -102.1 (d, $J = 251$, PHMe(Is) B). ^1H NMR (CD_2Cl_2): δ 7.72–7.70 (m, 2H, DuPhos Ar), 7.43–7.42 (m, 2H, DuPhos Ar), 7.02 (d, $J = 2$, 2H, Is Ar), 4.81 (dq, $J = 256$, 7, 1H, PH A), 4.74 (dq, $J = 251$, 7, 1H, PH B), 3.62–3.59 (br m, 2H, Is *i*-Pr CH), 2.86 (septet, $J = 7$, 1H, Is *i*-Pr CH), 2.48–2.46 (m, 2H, DuPhos CH), 2.30–2.23 (m, 2H, CH_2), 2.23–2.17 (m, 4H, 2H DuPhos CH + 2H CH_2), 2.00–1.95 (br, 2H, *i*-Pr CH), 1.80–1.71 (m, 2H, CH_2), 1.63–1.56 (m, 2H, *i*-Pr CH), 1.49–1.47 (m, 2H, CH_2), 1.39 (d, $J = 7$, 3H, P-Me A), 1.35 (d, $J = 7$, 3H, P-Me B), 1.25 + 1.23 (overlapping d, $J = 7$, 12H, Is *i*-Pr Me), 1.19 (apparent t, $J = 7$, 6H, Is *i*-Pr Me), 0.96 (d, $J = 7$, 6H, DuPhos *i*-Pr Me), 0.81 (d, $J = 7$, 6H, DuPhos *i*-Pr Me), 0.68 (d, $J = 7$, 6H, DuPhos *i*-Pr Me), 0.55 (d, $J = 7$, 6H, DuPhos *i*-Pr Me). $^{13}\text{C}\{^1\text{H}\}$ NMR (CD_2Cl_2): δ 152.2 (d, $J = 10$, quat Is A), 152.1 (d, $J = 10$, quat Is B), 149.5 (quat Is), 144.1 (t, $J = 21$, quat DuPhos), 134.4 (t, $J = 3$, DuPhos Ar), 129.0 (DuPhos Ar), 128.5 (d, $J = 16$, ipso quat Is), 121.5 (t, $J = 4$, Is), 52.1 (t, $J = 7$, DuPhos CH), 50.1 (t, $J = 7$, DuPhos CH), 34.3 (*i*-Pr CH), 32.44 (d, $J = 3$, *i*-Pr CH), 32.35 (d, $J = 3$, *i*-Pr CH), 31.3 (DuPhos CH_2), 30.7 (t, $J = 9$, *i*-Pr CH), 28.8 (DuPhos CH_2), 28.5 (*i*-Pr CH), 24.7 (*i*-Pr Me), 24.6 (*i*-Pr Me), 24.3 (*i*-Pr Me), 24.2 (*i*-Pr Me), 24.1 (t, $J = 4$, DuPhos *i*-Pr Me), 23.6 (d, $J = 3$, DuPhos *i*-Pr Me), 20.2 (DuPhos *i*-Pr Me), 19.8 (t, $J = 5$, DuPhos *i*-Pr Me), 8.2 (d, $J = 12$, P-Me).

NMR Data for $\text{Cu}((R,R)\text{-}i\text{-Pr-DuPhos})(\text{PHMe(Is)})(\text{Br})$ (11). $^{31}\text{P}\{^1\text{H}\}$ NMR (CD_2Cl_2): δ 4.6 (br, DuPhos), -100.5 (br, PHMe(Is) A), -102.3 (br, PHMe(Is) B), about 1:1 ratio. ^{31}P NMR (CD_2Cl_2): δ 4.6 (br, DuPhos), -100.5 (d, $J = 250$, PHMe(Is) A), -102.2 (d, $J = 252$, PHMe(Is) B). ^1H NMR (CD_2Cl_2): δ 7.71–7.70 (m, 2H, DuPhos Ar), 7.42–7.41 (m, 2H, DuPhos Ar), 7.02 (d, $J = 2$, 2H, Is Ar), 4.82 (dq, $J = 255$, 7, 1H, PH A), 4.74 (dq, $J = 250$, 7, 1H, PH B), 3.62–3.61 (br m, 2H, Is *i*-Pr CH), 2.86 (septet, $J = 7$, 1 H, Is *i*-Pr CH), 2.46–2.43 (m, 2H, DuPhos CH), 2.28–2.21 (m, 4H, 2H DuPhos CH + 2H CH_2), 2.21–2.13 (m, 2H, CH_2), 1.99 (br, 2H, CH_2), 1.77–1.70 (m, 2H, *i*-Pr CH), 1.61–1.53 (m, 4H, 2H CH_2 + 2H *i*-Pr CH), 1.41 (d, $J = 7$, 3H, P-Me A), 1.36 (d, $J = 7$, 3H, P-Me B), 1.25 + 1.23 (overlapping d, $J = 7$, 12H, Is *i*-Pr Me), 1.19 (apparent t, $J = 7$, 6H, Is *i*-Pr Me), 0.93 (d, $J = 7$, 6H, DuPhos *i*-Pr Me), 0.77 (d, $J = 7$, 6H, DuPhos *i*-Pr Me), 0.67 (d, $J = 7$, 6H, DuPhos *i*-Pr Me), 0.49 (d, $J = 7$, 6H, DuPhos *i*-Pr Me). $^{13}\text{C}\{^1\text{H}\}$ NMR (CD_2Cl_2): δ 152.2 (d, $J = 10$, quat Is A), 152.1 (d, $J = 10$, quat Is B), 149.7 (quat Is), 144.2 (t, $J = 21$, quat DuPhos), 134.4 (t, $J = 3$, DuPhos Ar), 129.1 (DuPhos Ar), 128.7 (d, $J = 16$, ipso quat Is), 121.5 (t, $J = 5$, Is), 52.1 (t, $J = 7$, DuPhos CH), 50.1 (t, $J = 7$, DuPhos CH), 34.3 (*i*-Pr CH), 32.45 (*i*-Pr CH), 32.37 (*i*-Pr CH), 30.9 (DuPhos CH_2), 30.7 (t, $J = 9$, *i*-Pr CH), 28.9 (DuPhos CH_2), 28.5 (*i*-Pr CH), 24.7 (*i*-Pr Me), 24.5 (*i*-Pr Me), 24.3 (*i*-Pr Me), 24.2 (*i*-Pr Me), 24.1 (t, $J = 3$, DuPhos *i*-Pr Me), 23.9 (t, $J = 4$, DuPhos *i*-Pr Me), 23.7 (*i*-Pr Me), 23.6 (br, *i*-Pr Me),

20.1 (t, $J = 4$, DuPhos *i*-Pr Me), 19.9 (DuPhos *i*-Pr Me), 8.2 (d, $J = 23$, P-Me).

NMR Data for $\text{Cu}((R,R)\text{-}i\text{-Pr-DuPhos})(\text{PHMe(Is)})(\text{I})$ (12). $^{31}\text{P}\{^1\text{H}\}$ NMR (CD_2Cl_2): δ 3.4 (br, DuPhos), -103.6 (br, PHMe(Is) A), -104.9 (br, PHMe(Is) B), about 1:1 ratio. ^{31}P NMR (CD_2Cl_2): δ 3.4 (br, DuPhos), -102.5 (overlapping d, $J = 274$, PHMe(Is) A), -104.5 (overlapping d, $J = 222$, PHMe(Is) B). ^1H NMR (CD_2Cl_2): δ 7.72–7.70 (m, 2H, DuPhos Ar), 7.44–7.42 (m, 2H, DuPhos Ar), 7.04 (d, $J = 2$, 2H, Is Ar), 4.74 (dq, $J = 246$, 7, 1H, PH A), 4.66 (dq, $J = 242$, 7, 1H, PH B), 3.66–3.65 (br m, 2H, Is *i*-Pr CH), 2.87 (septet, $J = 7$, 1 H, Is *i*-Pr CH), 2.48–2.44 (m, 2H, DuPhos CH), 2.27–2.25 (m, 4H, 2H DuPhos CH + 2H CH_2), 2.13–2.12 (m, 4H, CH_2), 1.78–1.71 (m, 2H, *i*-Pr CH), 1.62–1.57 (m, 4H, 2H CH_2 + 2H *i*-Pr CH), 1.40 (d, $J = 7$, 3H, P-Me A), 1.36 (d, $J = 7$, 3H, P-Me B), 1.28–1.20 (m, 18H, Is *i*-Pr Me), 0.93 (d, $J = 7$, 6H, DuPhos *i*-Pr Me), 0.78 (d, $J = 7$, 6H, DuPhos *i*-Pr Me), 0.66 (d, $J = 7$, 6H, DuPhos *i*-Pr Me), 0.46 (d, $J = 7$, 6H, DuPhos *i*-Pr Me). $^{13}\text{C}\{^1\text{H}\}$ NMR (CD_2Cl_2): δ 152.4–152.2 (m, quat Is), 149.74 (quat Is), 149.71 (quat Is), 144.1 (t, $J = 21$, quat DuPhos), 134.4 (t, $J = 3$, DuPhos Ar), 129.1 (DuPhos Ar), 121.5–121.4 (m, Is), 52.3 (t, $J = 7$, DuPhos CH), 50.4 (t, $J = 7$, DuPhos CH), 34.3 (*i*-Pr CH), 32.5–32.3 (m, *i*-Pr CH), 30.6 (br, DuPhos CH_2), 29.0 (DuPhos CH_2), 28.5 (*i*-Pr CH), 24.7 (DuPhos *i*-Pr Me), 24.5 (DuPhos *i*-Pr Me), 24.3 (*i*-Pr Me), 24.2 (*i*-Pr Me), 24.3–24.0 (m, *i*-Pr Me), 23.7 (*i*-Pr Me), 23.6 (*i*-Pr Me), 20.5 (t, $J = 4$, DuPhos *i*-Pr Me), 19.7 (DuPhos *i*-Pr Me), 8.7 (d, $J = 26$, P-Me A), 8.5 (d, $J = 30$, P-Me B). The quaternary ipso P–Is signal was not observed.

General Procedure for Isolation of $\text{Cu}((R,R)\text{-}i\text{-Pr-DuPhos})(\text{PHMe(Is)})(\text{X})$ (10 and 11) and Attempted Isolation of Iodide Analogue 12. To a slurry of CuX (0.23 mmol; 23 mg of CuCl, 33 mg of CuBr, or 44 mg of CuI) in 2 mL of THF was added a solution of $(R,R)\text{-}i\text{-Pr-DuPhos}$ (96 mg, 0.23 mmol) in 2 mL of THF, and the resulting solution (yellow, green, or yellow, respectively, depending on the halide) was stirred for 20 min. A solution of PHMe(Is) (57 mg, 0.23 mmol, or 115 mg, 0.46 mmol, for the iodide complex) in 2 mL of THF was added, and the solution was stirred for 10 min. The solution was filtered through Celite and concentrated under vacuum to give a yellow, yellow-green, or pale yellow powder, respectively. The solid was partially redissolved in ether (~3 mL) at room temperature and then cooled to $-20\text{ }^\circ\text{C}$ to give a crystalline solid, either yellow, yellow-green, or pale yellow, respectively. The solution was decanted, and the crystals were dried under vacuum. X-ray crystallography showed that the crystals were 10, 11, and $[\text{Cu}((R,R)\text{-}i\text{-Pr-DuPhos})(\text{I})]_2$, respectively.

$\text{Cu}((R,R)\text{-}i\text{-Pr-DuPhos})(\text{PHMe(Is)})(\text{I})$ (13). To $[\text{Cu}((R,R)\text{-}i\text{-Pr-DuPhos})(\text{I})]_2$ (20 mg, 0.017 mmol) was added a solution of PHMe(Is) (8 mg, 0.03 mmol) in 2 mL of THF. The resulting orange solution was stirred for 10 min and then concentrated under vacuum to give an orange oil (32 mg, 114%, excess PHMe(Is) present) which contained two diastereomers (A:B, 55:45).

$^{31}\text{P}\{^1\text{H}\}$ NMR (CDCl_3 , $25\text{ }^\circ\text{C}$): δ 2.5 (Me-FerroLANE), -103.9 (PHMe(Is) A), -104.5 (PHMe(Is) B). ^1H NMR (CDCl_3): δ 6.94 (d, $J = 2$, 2H, Is CH), 4.72 (dq, $J = 249$, 7, 1H, PH A), 4.67 (dq, $J = 244$, 7, 1H, PH B), 4.44 (2H, Cp), 4.36 (br, 2H, Cp), 4.23 (br, 2H, Cp), 4.10 (2H, Cp), 3.58–3.52 (m, 2H, *i*-Pr CH), 2.81–2.77 (m, 1H, *i*-Pr CH), 2.65–2.60 (m, 2H, FerroLANE CH), 2.31–2.25 (m, 2H, CH_2), 2.16–2.11 (m, 2H, CH_2), 1.91–1.86 (m, 2H, FerroLANE CH), 1.50–1.46 (m, 6H, FerroLANE Me), 1.40–1.30 (br m, 2H, CH_2), 1.35 (br d, $J = 7$, P-Me A), 1.31 (br d, $J = 7$, P-Me B), 1.25–1.20 (br m, 2H, CH_2), 1.21 (t, $J = 6$) and 1.19–1.15 (m, 18H total, *i*-Pr Me), 0.85–0.82 (app. q, $J = 7$, 6H, FerroLANE Me). $^{13}\text{C}\{^1\text{H}\}$ NMR (CDCl_3): δ 152.2 (d, $J = 10$, quat *o*-Is B), 152.0 (d, $J = 10$, quat *o*-Is A), 149.5 (quat *p*-Is), 121.5 (t, $J = 4$, *m*-Is CH), 76.5 (t, $J = 11$, Cp CH), 73.6 (t, $J = 10$, quat Cp), 73.0 (t, $J = 3$, Cp CH), 70.9 (Cp CH), 70.1 (Cp CH), 35.7 (CH_2), 35.1 (CH_2), 35.0 (t, $J = 9$, FerroLANE CH), 34.2 (d, $J = 3$, *i*-Pr CH), 34.0 (t, $J = 9$, FerroLANE CH), 32.7 (d, $J = 12$, *i*-Pr CH), 32.6 (d, $J = 13$, *i*-Pr CH), 25.0 (*i*-Pr Me), 24.8 (*i*-Pr Me), 24.6 (*i*-Pr Me), 24.5 (*i*-Pr Me), 23.9 (*i*-Pr Me), 21.0 (t, $J = 9$, FerroLANE Me), 15.3 (FerroLANE Me), 8.56 (d, $J = 63$, P-Me A), 8.55 (d, $J = 66$, P-Me B, overlapping). One quaternary aryl carbon signal was not observed.

Generation of Cu((R,R)-i-Pr-DuPhos)(PMels) (14) from Cation 6. Separate solutions of [Cu((R,R)-i-Pr-DuPhos)(NCMe)(PHMeIs)]⁺[PF₆]⁻ (6, 10 mg, 0.01 mmol) in 0.5 mL of THF and NaOSiMe₃ (2 mg, 0.02 mmol, 2 equiv) in 0.5 mL of THF were prepared in NMR tubes with septa caps, which were cooled to -78 °C in a dry ice/acetone bath. The solution of NaOSiMe₃ was transferred via cannula into the solution of the copper complex, which was kept at -78 °C until it was placed in a precooled NMR probe at -70 °C and then slowly warmed to room temperature. ³¹P{¹H} NMR (THF): δ 7.6 (d, J = 90, minor 14 DuPhos), 5.0 (d, J = 94, major 14 DuPhos, 1:4 ratio), 3.0 (very br, DuPhos in Cu((R,R)-i-Pr-DuPhos)(PHMe(Is))(OSiMe₃) (15)), -10.7 (br, [Cu((R,R)-i-Pr-DuPhos)(OSiMe₃)_n (16)], -12.4 (i-Pr-DuPhos), -107.2 (t, J = 94, major 14 PMels), -109 (br, minor 14 PMels), -111.1, -111.2 (two diastereomers of 15).

Generation of Cu((R,R)-i-Pr-DuPhos)(PMels) (14) from Bromide Complex 11. To a solution in 1 mL of THF of freshly recrystallized [Cu((R,R)-i-Pr-DuPhos)(Br)]₂ prepared from CuBr (20 mg, 0.14 mmol) and (R,R)-i-Pr-DuPhos (59 mg, 0.14 mmol) was added PHMe(Is) (35 mg, 0.14 mmol). The resulting green solution was treated with NaOSiMe₃ (20 mg, 0.18 mmol, 1.3 equiv). The ³¹P{¹H} NMR spectrum showed signals assigned to the two diastereomers of 14 (1:4 ratio; δ 7.3 (d, J = 91, minor DuPhos), 4.8 (d, J = 91, major DuPhos), -107.3 (t, J = 91, PMels)), [Cu((R,R)-i-Pr-DuPhos)(OSiMe₃)_n (16, δ -10.5), and two diastereomers of Cu((R,R)-i-Pr-DuPhos)(PHMe(Is))(OSiMe₃) (15), which was the major species present (δ 5.5 (br, DuPhos), -108.4 (br, J_{PH} = 229, PHMe(Is), -110.1 (J_{PH} = 216, PHMe(Is)). A little i-Pr-DuPhos (δ -12.5) and a minor unidentified species (δ 10.5) were also observed.

[Cu((R,R)-i-Pr-DuPhos)(OSiMe₃)_n (16). To CuCl (20 mg, 0.2 mmol) was added a solution of (R,R)-i-Pr-DuPhos (84 mg, 0.2 mmol) in 1 mL of THF. The yellow-green solution was filtered through Celite; the solvent was removed in vacuo, and the yellow-green solid was recrystallized from ether at -30 °C. The resulting yellow solid was washed with ether (2 × 2 mL) to give a yellow powder (81 mg, 0.08 mmol). To the yellow solid was added NaOSiMe₃ (18 mg, 0.16 mmol, 1 equiv per Cu) in 1 mL of THF, resulting in a bright yellow-orange solution. A white solid formed as the reaction progressed over about 5 min. An initial ³¹P{¹H} NMR spectrum revealed incomplete conversion (unidentified byproduct δ -6.8, 8%), so additional NaOSiMe₃ (5 mg, 0.04 mmol) was added, resulting in complete conversion to the product (δ -10.2). The solution was filtered through Celite, and solvent was removed in vacuo to give an orange oil (87.5 mg, 98%).

³¹P{¹H} NMR (C₆D₆): δ -10.2. ¹H NMR (C₆D₆): δ 7.40–7.38 (m, 4H, Ar), 7.04–7.03 (m, 4H, Ar), 2.31–2.26 (m, 4H, DuPhos CH), 2.24–2.17 (m, 4H, DuPhos CH), 2.16–2.09 (m, 4H, i-Pr CH), 1.99–1.88 (m, 8H, 4H i-Pr CH + 4H CH₂), 1.56–1.49 (m, 4H, CH₂), 1.45–1.37 (m, 4H, CH₂), 1.23 (d, J = 7, 12H, Me), 1.21–1.15 (m, 4H, CH₂), 1.00 (d, J = 7, 12H, Me), 0.74 (d, J = 7, 12H, Me), 0.69 (d, J = 7, 12H, Me), 0.42 (9H, OSiMe₃). ¹³C{¹H} NMR (C₆D₆): δ 144.4 (t, J = 22, quat Ar), 134.4 (Ar CH), 129.2 (Ar CH), 53.1 (t, J = 8, DuPhos CH), 51.4 (t, J = 8, DuPhos CH), 33.4 (CH₂), 31.0 (t, J = 9, i-Pr CH), 29.2 (i-Pr CH), 28.6 (CH₂), 25.0 (br, Me), 24.1 (t, J = 5, Me), 21.8 (t, J = 4, Me), 19.9 (t, J = 4, Me), 4.8 (OSiMe₃).

Reaction of [Cu((R,R)-i-Pr-DuPhos)(OSiMe₃)_n (16) with PHMe(Is). To [Cu((R,R)-i-Pr-DuPhos)(OSiMe₃)_n (8 mg, 0.007 mmol of a dimer) was added a solution of PHMe(Is) (5 mg, 0.02 mmol, 1.4 equiv per Cu) in 1 mL of THF, resulting in a yellow-orange solution. The ³¹P{¹H} NMR spectrum showed signals assigned to the two diastereomers of 14 (1:4 ratio; δ 7.6 (d, J = 90, minor DuPhos), 5.0 (d, J = 94, major DuPhos), -106.8 (t, J = 94, major PMels), -109.2 (br t, J = 90, minor PMels), 16 (δ -10.5), and 15 (δ 5.5 (br, DuPhos), -111.2 (br, J_{PH} = 211, PHMe(Is)); individual signals of the two diastereomers were not observed, presumably because of exchange with PHMe(Is). A small amount of i-Pr-DuPhos (δ -12.5) and an unidentified byproduct (δ 8.0) were also observed.

Generation of Cu((R,R)-Me-FerroLANE)(PMels) (17) from Cation 7. To a solution of [Cu((R,R)-Me-FerroLANE)(PHMe-

(Is)]⁺[PF₆]⁻ (7, 15 mg, 0.02 mmol) in 1 mL of THF was added a solution of NaOSiMe₃ (5 mg, 0.04 mmol, 2 equiv) in 0.5 mL of THF at room temperature. The resulting orange solution was monitored by ³¹P{¹H} NMR spectroscopy, which showed signals due to both diastereomers of 17, along with Me-FerroLANE and PHMe(Is). In a similar experiment, deprotonation was carried out at -78 °C, and spectra were acquired at low temperature.

³¹P{¹H} NMR (THF, 25 °C): δ 10.6 (d, J = 115, FerroLANE A (major)), 9.5 (br, FerroLANE B), -1.0 (Me-FerroLANE), -94.0 (d, J = 115, PMels A), -97.8 (br, PMels B), -111.2 (PHMe(Is)), -142.4 (sp, J = 710, PF₆). Selected ³¹P NMR (THF, 25 °C): δ -111.2 (d, J = 208, PHMe(Is)). ³¹P{¹H} NMR (THF-d₈, -35 °C): δ 10.2 (d, J = 114, FerroLANE A), 8.8 (d, J = 110, FerroLANE B), -94.9 (t, J = 114, PMels A), -98.9 (t, J = 110, PMels B), -112.1 (PHMe(Is), -143.1 (sp, J = 708, PF₆).

■ ASSOCIATED CONTENT

● Supporting Information

The Supporting Information is available free of charge on the ACS Publications website at DOI: 10.1021/acs.inorgchem.9b01263.

Additional experimental information, NMR spectra, and details of the X-ray crystallographic and computational studies (PDF)

Accession Codes

CCDC 1908340–1908345 contain the supplementary crystallographic data for this paper. These data can be obtained free of charge via www.ccdc.cam.ac.uk/data_request/cif, by emailing data_request@ccdc.cam.ac.uk, or by contacting The Cambridge Crystallographic Data Centre, 12 Union Road, Cambridge CB2 1EZ, UK; fax: +44 1223 336033.

■ AUTHOR INFORMATION

Corresponding Author

*E-mail: glueck@dartmouth.edu.

ORCID

Matthew F. Cain: 0000-0002-0673-5839

Russell P. Hughes: 0000-0002-1891-6530

David S. Glueck: 0000-0002-8438-8166

Notes

The authors declare no competing financial interest.

■ ACKNOWLEDGMENTS

We thank the National Science Foundation (Grants CHE-126578, -1562037, and -1011887) and Dartmouth College for support and the Department of Education for GAANN fellowship support to M.F.C.

■ REFERENCES

- (1) Nell, B. P.; Tyler, D. R. Synthesis, reactivity, and coordination chemistry of secondary phosphines. *Coord. Chem. Rev.* **2014**, *279*, 23–42.
- (2) For A, see: (a) Black, J. R.; Levason, W.; Spicer, M. D.; Webster, M. Synthesis and Solution Multinuclear Magnetic Resonance Studies of Homoleptic Copper(I) Complexes of Group 15 Donor Ligands. *J. Chem. Soc., Dalton Trans.* **1993**, 3129–3136. for B, see (b) Abel, E. W.; McLean, R. A. N.; Sabherwal, I. H. Synthetic and spectroscopic studies on diphenylphosphine complexes of copper(I). *J. Chem. Soc. A* **1969**, 133–136.
- (3) For related Cu(I) secondary phosphine complexes, see: (a) Kang, Y. B.; Pabel, M.; Pathak, D. D.; Willis, A. C.; Wild, S. B. Copper(I)-Facilitated Methylation and Cyclic Alkylation of 1,2-Phenylenebis(phosphine). *Main Group Chem.* **1995**, *1*, 89–98. (b) Doel, C. L.; Gibson, A. M.; Reid, G.; Frampton, C. S. Synthesis

and multinuclear NMR studies on copper and silver complexes of multidentate phosphine and mixed phospho/thia ligands. Single crystal structure of $[\text{Cu}(\text{P}_2\text{S}_2)]\text{PF}_6$ ($\text{P}_2\text{S}_2 = \text{Ph}_2\text{PCH}_2\text{CH}_2\text{SCH}_2\text{CH}_2\text{-SCH}_2\text{CH}_2\text{PPh}_2$). *Polyhedron* **1995**, *14*, 3139–3146. (c) Böttcher, H.-C.; Graf, M.; Merzweiler, K.; Bruhn, C. Reaction of $[\{\text{CuCl}(\text{Bu}_2\text{PH})\}_4]$ with $[\text{Ru}_3(\text{CO})_{12}]$: X-ray crystal structures of the chloride transfer products $[\text{Ru}_3(\text{CO})_7(\mu\text{-H})(\mu\text{-PBu}_2)_2(\mu\text{-Cl})]$ and the electron-rich 50-electron cluster $[\text{Ru}_3(\text{CO})_6(\mu\text{-PBu}_2)_3(\mu\text{-Cl})_3(\text{Bu}_2\text{PH})]$. *Polyhedron* **1997**, *16*, 3253–3260. (d) Azizpoor Fard, M.; Rabiee Kenaree, A.; Boyle, P. D.; Ragogna, P. J.; Gilroy, J. B.; Corrigan, J. F. Coinage metal coordination chemistry of stable primary, secondary and tertiary ferrocenylethyl-based phosphines. *Dalton Trans.* **2016**, *45*, 2868–2880. (e) Brüllingen, E.; Neudörf, J.-M.; Goldfuss, B. Enantioselective Cu-catalyzed 1,4-additions of organozinc and Grignard reagents to enones: exceptional performance of the hydrido-phosphite-ligand BIFOP-H. *New J. Chem.* **2019**, *43*, 4787–4799.

(4) Lambert, B.; Desreux, J. F. Synthesis of Macrocyclic Polyphosphine Oxides and Phosphines by Template Cyclisation and Demetallation. *Synthesis* **2000**, *2000*, 1668–1670.

(5) Nell, B. P.; Swor, C. D.; Henle, E. A.; Zakharov, L. N.; Rinehart, N. I.; Nathan, A.; Tyler, D. R. Synthesis of tetraphosphine macrocycles using copper(I) templates. *Dalton Trans.* **2016**, *45*, 8253–8264.

(6) Cain, M. F.; Hughes, R. P.; Glueck, D. S.; Golen, J. A.; Moore, C. E.; Rheingold, A. L. Synthesis and Structure of Intermediates in Copper-Catalyzed Alkylation of Diphenylphosphine. *Inorg. Chem.* **2010**, *49*, 7650–7662.

(7) (a) Kolodiazny, O. I. *Asymmetric Synthesis in Organophosphorus Chemistry: Synthetic Methods, Catalysis, and Applications*; Wiley-VCH: Weinheim, 2016. (b) Grabulosa, A. *P-Stereogenic Ligands in Enantioselective Catalysis*; RSC: Cambridge, 2011. (c) Glueck, D. S. Catalytic Asymmetric Synthesis of Chiral Phosphanes. *Chem. - Eur. J.* **2008**, *14*, 7108–7117. (d) Glueck, D. S. Recent Advances in Metal-Catalyzed C–P Bond Formation. *Top. Organomet. Chem.* **2010**, *31*, 65–100. (e) Glueck, D. S. Metal-Catalyzed Asymmetric Synthesis of P-Stereogenic Phosphines. *Synlett* **2007**, *2007*, 2627–2634.

(8) *Catalysis Without Precious Metals*; Bullock, R. M., Ed.; Wiley-VCH: Weinheim, 2010.

(9) (a) Burk, M. J. Modular Phospholane Ligands in Asymmetric Catalysis. *Acc. Chem. Res.* **2000**, *33*, 363–372. (b) Guino-O, M. A.; Zureick, A. H.; Blank, N. F.; Anderson, B. J.; Chapp, T. W.; Kim, Y.; Glueck, D. S.; Rheingold, A. L. Synthesis and Structure of Platinum Bis(phospholane) Complexes $\text{Pt}(\text{diphos}^*)(\text{R})(\text{X})$, Catalyst Precursors for Asymmetric Phosphine Alkylation. *Organometallics* **2012**, *31*, 6900–6910.

(10) (a) Bader, A.; Pabel, M.; Wild, S. B. First Resolution of a Free Secondary Phosphine Chiral at Phosphorus. *J. Chem. Soc., Chem. Commun.* **1994**, 1405–1406. (b) Bader, A.; Nullmeyers, T.; Pabel, M.; Salem, G.; Willis, A. C.; Wild, S. B. Stereochemistry and Stability of Free and Coordinated Secondary Phosphines. Crystal and Molecular Structure of $[\text{S}-(\text{R}^*,\text{R}^*),(\text{R}^*)]-(+)\text{S}_{89}\text{-[PtCl}\{1,2\text{-C}_6\text{H}_4(\text{PMePh})_2\}(\text{PHMePh})\text{PF}_6\cdot\text{CH}_2\text{Cl}_2]$. *Inorg. Chem.* **1995**, *34*, 384–389. (c) Bader, A.; Pabel, M.; Willis, A. C.; Wild, S. B. First Resolution of a Free Secondary Phosphine Chiral at Phosphorus and Stereospecific Formation and Structural Characterization of a Homochiral Secondary Phosphine-Borane Complex. *Inorg. Chem.* **1996**, *35*, 3874–3877. (d) Wicht, D. K.; Kovacic, I.; Glueck, D. S.; Liable-Sands, L. M.; Incarvito, C. D.; Rheingold, A. L. Chiral Terminal Platinum(II) Phosphido Complexes: Synthesis, Phosphorus Inversion, and Acrylonitrile Insertion. *Organometallics* **1999**, *18*, 5141–5151. (e) Albert, J.; Magali Cadena, J.; Granell, J.; Muller, G.; Panyella, D.; Sañudo, C. Resolution of Secondary Phosphanes Chiral at Phosphorus by Means of Palladium Metallacycles. *Eur. J. Inorg. Chem.* **2000**, *2000*, 1283–1286. (f) Huang, Y.; Li, Y.; Leung, P.-H.; Hayashi, T. Asymmetric Synthesis of P-Stereogenic Diarylphosphinites by Palladium-Catalyzed Enantioselective Addition of Diarylphosphines to Benzoquinones. *J. Am. Chem. Soc.* **2014**, *136*, 4865–4868.

(11) (a) Rogers, J. R.; Wagner, T. P. S.; Marynick, D. S. Metal-Assisted Pyramidal Inversion in Metal-Phosphido Complexes. *Inorg. Chem.* **1994**, *33*, 3104–3110. (b) Glueck, D. S. Applications of ^{31}P NMR Spectroscopy in Development of M(Duphos)-Catalyzed Asymmetric Synthesis of P-Stereogenic Phosphines (M = Pt or Pd). *Coord. Chem. Rev.* **2008**, *252*, 2171–2179. Glueck, D. S. Erratum to “Applications of ^{31}P NMR spectroscopy in development of M(Duphos)-catalyzed asymmetric synthesis of P-stereogenic phosphines (M = Pt or Pd)” [*Coord. Chem. Rev.* *252* (2008) 2171–2179]. *Coord. Chem. Rev.* **2011**, *255*, 356.

(12) Wang, G.; Gibbons, S. K.; Glueck, D. S.; Sibbald, C.; Fleming, J. T.; Higham, L. J.; Rheingold, A. L. Copper–Phosphido Intermediates in Cu(IPr)-Catalyzed Synthesis of 1-Phosphapyracenes via Tandem Alkylation/Arylation of Primary Phosphines. *Organometallics* **2018**, *37*, 1760–1772.

(13) Related $[\text{Cu}(\text{diphos})(\text{NCMe})_n]^+$ complexes contain one or two coordinated acetonitrile ligands. For $[\text{Cu}(\text{dppf})(\text{NCMe})_2]^+$, see: (a) Díez, J.; Gamasa, M. P.; Gimeno, J.; Aguirre, A.; García-Granda, S.; Holubova, J.; Falvello, L. R. Novel Copper(I) Complexes Containing 1,1'-Bis(diphenylphosphino)ferrocene (dppf) as a Chelate and Bridging Ligand: Synthesis of Tetrabridged Dicopper(I) Complexes $[\text{Cu}_2(\mu\text{-}\eta^1\text{-C:CR})_2(\mu\text{-dppf})_2]$ and X-ray Crystal Structure of $[\text{Cu}_2(\mu\text{-}\eta^1\text{-C:CC}_6\text{H}_4\text{CH}_3)_2(\mu\text{-dppf})_2]$. *Organometallics* **1999**, *18*, 662–669. (b) Kim, H.-S.; Kim, J.-W.; Kwon, S.-C.; Shim, S.-C.; Kim, T.-J. Catalytic formation of carbamates and cyclic carbonates by copper complex of 2,5,19,22-tetraaza[6,6](1,1')ferrocenophane-1,5-diene X-ray crystal structure of $[\text{Cu}(\text{I})\text{PF}_6]$. *J. Organomet. Chem.* **1997**, *545–546*, 337–344. The crystal structures of both $[\text{Cu}(\text{Xantphos})(\text{NCMe})]^+$ and $[\text{Cu}(\text{Xantphos})(\text{NCMe})_2]^+$ have been reported; see: ref 6 and (c) Yuasa, J.; Dan, M.; Kawai, T. Phosphorescent properties of metal-free diphosphine ligands and effects of copper binding. *Dalton Trans.* **2013**, *42*, 16096–16101.

(14) (a) Burk, M. J.; Feaster, J. E.; Nugent, W. A.; Harlow, R. L. Preparation and Use of C_2 -Symmetric Bis(phospholanes): Production of α -Amino Acid Derivatives via Highly Enantioselective Hydrogenation Reactions. *J. Am. Chem. Soc.* **1993**, *115*, 10125–10138. (b) Marinho, V. R.; Ramalho, J. P. P.; Rodrigues, A. I.; Burke, A. J. A Comparison of (R,R)-Me-DUPHOS and (R,R)-DUPHOS-*i*Pr Ligands in the Pd^0 -Catalyzed Asymmetric Allylic Alkylation Reaction: Stereochemical and Kinetic Considerations. *Eur. J. Org. Chem.* **2010**, *2010*, 1593.

(15) Moudam, O.; Kaeser, A.; Delavaux-Nicot, B.; Duhayon, C.; Holler, M.; Accorsi, G.; Armadori, N.; Séguy, I.; Navarro, J.; Destruel, P.; Nierengarten, J.-F. Electrophosphorescent Homo- and Heteroleptic Copper(I) Complexes Prepared from Various Bis-phosphine Ligands. *Chem. Commun.* **2007**, 3077–3079.

(16) Cain, M. F.; Reynolds, S. C.; Anderson, B. J.; Glueck, D. S.; Golen, J. A.; Moore, C. E.; Rheingold, A. L. Synthesis, Structure and Spectroscopic Properties of 2,3-bis(diphenylphosphino)quinoxaline (dppQx) and Its Copper(I) Complexes. *Inorg. Chim. Acta* **2011**, *369*, 55–61.

(17) Gibbons, S. K.; Hughes, R. P.; Glueck, D. S.; Royappa, A. T.; Rheingold, A. L.; Arthur, R. B.; Nicholas, A. D.; Patterson, H. H. Synthesis, Structure, and Luminescence of Copper(I) Halide Complexes of Chiral Bis(phosphines). *Inorg. Chem.* **2017**, *56*, 12809–12820.

(18) It is noteworthy that the bridging Me-FerroLANE observed in the crystal structure¹⁷ of $[\text{Cu}(\text{Me-FerroLANE})(\text{I})]_2$ was converted to a chelate in secondary phosphine adduct 13.

(19) As observed previously in reactions of Cu(I) with phosphines, in some cases, unidentified phosphine oxides were formed, perhaps via oxidations mediated by Cu(II) impurities. This was especially problematic for 9, which we could not isolate in pure form, and also occurred in generation of 10–12. See ref 17 and (a) Côté, A.; Boezio, A. A.; Charette, A. B. Evidence for the Structure of the Enantioactive Ligand in the Phosphine-Copper-Catalyzed Addition of Diorganozinc Reagents to Imines. *Angew. Chem., Int. Ed.* **2004**, *43*, 6525–6528. (b) Berners-Price, S. J.; Johnson, R. K.; Mirabelli, C. K.; Faucette, L. F.; McCabe, F. L.; Sadler, P. J. Copper(I) complexes with bidentate

tertiary phosphine ligands: solution chemistry and antitumor activity. *Inorg. Chem.* **1987**, *26*, 3383–3387. (c) Ferraris, D.; Young, B.; Cox, C.; Drury, W. J.; Dudding, T.; Lectka, T. Diastereo- and Enantioselective Alkylation of α -Imino Esters with Enol Silanes Catalyzed by (R)-Tol-BINAP-CuClO₄·(MeCN)₂. *J. Org. Chem.* **1998**, *63*, 6090–6091.

(20) Burk, M. J.; Gross, M. F. New Chiral 1,1'-Bis(phospholano)-ferrocene Ligands for Asymmetric Catalysis. *Tetrahedron Lett.* **1994**, *35*, 9363–9366.

(21) Brauer, D. J.; Bitterer, F.; Dorrenbach, F.; Hessler, G.; Stelzer, O.; Kruger, C.; Lutz, F. Synthesis, Coordination Chemistry and Ligand Properties of Secondary Phosphines R(Ar*)PH with Bulky Aromatic Substituents – Molecular Structure of Ph(Is)PH, Is₂PH and ClAu[PhPMe*H]. *Z. Naturforsch., B: J. Chem. Sci.* **1996**, *51*, 1183–1196.

(22) Ozdemir, N.; Dincer, M.; Dayan, O.; Cetinkaya, B. (Acetonitrile){2,6-bis[1-(2,4,6-trimethylphenylimino)ethyl]pyridine}-dichloridoruthenium(II) dichloromethane solvate. *Acta Crystallogr., Sect. C: Cryst. Struct. Commun.* **2007**, *63*, m407–m409.

(23) Szymanska, I. ⁶³Cu and ³¹P Nuclear Magnetic Resonance for Characterization of Cu(I) Complexes with P-Donor Ligands. *Polish. J. Chem.* **2006**, *80*, 1095–1117.

(24) Complex **16** could contain terminal or bridging silanolates; the similarity of its ³¹P NMR chemical shift to those of the halides [Cu((R,R)-i-Pr-DuPhos)(X)]₂ (ref 17) is consistent with an analogous dimeric structure. For related Cu(I) phosphine silanolate complexes, see: (a) Schmidbaur, H.; Adlkofer, J.; Shiotani, A. Heterosiloxane des Kupfers, Silbers und Golds. *Chem. Ber.* **1972**, *105*, 3389–3396. (b) McGearry, M. J.; Wedlich, R. C.; Coan, P. S.; Folting, K.; Caulton, K. G. Synthesis and thermal decomposition of copper(I) silyloxy complexes. X-ray crystal structures of [Cu(OSiPh₃)₄]₂ and [Cu(OSiPh₃)(PMe₂Ph)]₂. *Polyhedron* **1992**, *11*, 2459–2473.

(25) Pangborn, A. B.; Giardello, M. A.; Grubbs, R. H.; Rosen, R. K.; Timmers, F. J. Safe and Convenient Procedure for Solvent Purification. *Organometallics* **1996**, *15*, 1518–1520.

(26) Kubas, G. J. Tetrakis(acetonitrile)Copper(1+) Hexafluorophosphate(1-). *Inorg. Synth.* **2007**, *28*, 68–70.